

W 4 C748p 2003
Confer, Nils F.
Protein-protein interactions
between poly(ADP-ribose)

UNTHSC - FW



M03N9B

LEWIS LIBRARY
UNT Health Science Center
3500 Camp Bowie Blvd.
Ft. Worth, Texas 76107-2699

Confer, Nils Forgard, Protein-Protein Interactions Between Poly(ADP-ribose) Polymerase-1 and DNA Polymerase β . Doctor of Philosophy (Biomedical Sciences), December 2003, 114 Pages, 22 Figures, 1 Graph, and 80 References.

The mammalian genome is continually subjected to chemical and environmental modifications that are repaired by base excision, and when excessive, may lead to apoptosis. Interestingly, the chromosomal enzyme poly(ADP-ribose) polymerase-1 (PARP-1) appears to modulate both mechanisms, either facilitating DNA repair and/or modulating cell death. In this dissertation project, experiments were performed to address the regulatory potential of PARP-1 in base excision repair (BER) and specifically on DNA polymerase β (pol β) function. Activity gels were used to measure the DNA polymerase activity of pol β following protein-(ADP-ribosyl)ation. However, the fraction of pol β molecules poly(ADP-ribosyl)ated was never 100% under the reaction conditions employed. In fact, similar results were observed in activity gels specific for PARP-1, even under conditions where this polymerase is the primary nuclear acceptor for poly(ADP-ribose). Here, I also describe a newly developed electrophoretic-mobility-shift-assay (EMSA) to monitor for the specific binding of pol β to a custom-made five-nucleotide gapped DNA duplex. However, while specific for pol β , this assay was inefficient to monitor the effects of covalent poly(ADP-ribosyl)ation on pol β activity. Moreover, I also observed the specific molecular association of PARP-1 with pol β by co-immunoprecipitation experiments, followed by reciprocal immuno-blotting for the protein partner. Knowing that during apoptosis endogenous PARP-1 is specifically proteolyzed into two peptide fragments by caspases, conditions were established for the

efficient proteolysis of PARP-1 by either caspase-3 and/or caspase-7. Experimental results indicated that caspase-3 was more efficient than caspase-7 at splitting unmodified PARP-1 into two peptide fragments. By contrast, caspase-7 appeared best suited for the proteolysis of covalently auto-poly(ADP-ribosyl)ated-(PARP-1). Interestingly, both of the caspase-generated peptide fragments of PARP-1 specifically associated with pol β as supported by co-immunoprecipitation/immuno-blotting experiments. Taken together, the experimental results presented here support the hypothesis that a molecular mechanism exists that involves interaction(s) of PARP-1 with pol β that may help to facilitate the decision making process between cell survival and cell death. Thus, upon proteolytic degradation of PARP-1 into a 24-kDa amino-terminal fragment and an 89-kDa carboxy-terminus, each truncated peptide, separately, retains physical association with pol β , and inhibits DNA repair associated pol β activity to irreversibly switch the fate of the cell from BER toward chromatin degradation and, eventually, programmed cell death.

PROTEIN-PROTEIN INTERACTIONS BETWEEN POLY(ADP-RIBOSE)

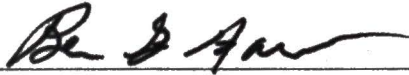
POLYMERASE-1 AND DNA POLYMERASE β

Nils F. Confer B.S.

Approved:



Major Professor



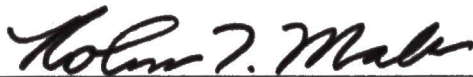
Committee Member



Committee Member



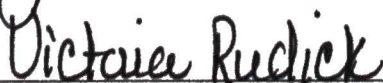
Committee Member



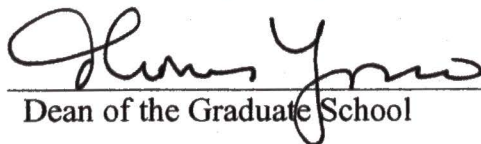
Committee Member



University Member



Graduate Advisor of Biomedical Sciences



Dean of the Graduate School

PROTEIN-PROTEIN INTERACTIONS BETWEEN POLY(ADP-RIBOSE)

POLYMERASE-1 AND DNA POLYMERASE β

DISSERTATION

**Presented to the Graduate Council of the
Graduate School of Biomedical Sciences**

University of North Texas

Health Science Center at Fort Worth

In Partial Fulfillment of the Requirements

For the Degree of

DOCTOR OF PHILOSOPHY

By

Nils F. Confer, B.S.

Fort Worth, Texas

December, 2003

TABLE OF CONTENTS

	Page
Acknowledgments	iii
List of Illustrations	vii
List of Abbreviations	ix
Chapter	
I. Introduction	
Opening Statement	1
Base Excision Repair	3
DNA Polymerase β	7
Poly(ADP-ribose) polymerase-1	15
Caspases	21
Research Prospectus	26
II. Materials and Methods	
Materials	29
Purification of PARP-1	29
Isolation of Rat Liver Chromatin	30
Cell Culture	31
Comet Assay	31
Auto-Poly(ADP-ribosyl)ation of PARP-1	32

Activity Gels	33
Proteolytic Digestion of Proteins by Caspases	34
Co-Immunoprecipitation of PARP-1 Peptides with DNA Polymerase β	34
Western Blotting	35
Electrophoretic Mobility Shift Assay	36
Tryptic Digestion of DNA Polymerase β	36
III. Results	
The Comet Assay	38
Experimental Design to Generate a DNA Substrate for DNA Polymerase β Binding	40
Electrophoretic Mobility Shift Assays Specific for DNA Polymerase β	40
DNA Polymerase β -Specific Activity Gel Assay	42
Activity Gels with DNA Polymerase β Following Protein-poly(ADP-ribosyl)ation	43
DNA Polymerase β Activity Gels with Chromatin Extracts Following Covalent Poly(ADP- ribosyl)ation	43
Poly(ADP-ribosyl)ation of Chromatin Proteins	44
PARP-1 Activity Gel Assay	45
Co-Immunoprecipitation of PARP-1 with DNA	

	Polymerase β	46
	Proteolysis of PARP-1 with Caspases	47
	Proteolysis of PARP-1 with Caspases Following Poly(ADP-ribosyl)ation	48
	Proteolysis of Chromatin Proteins with Caspases Following Poly(ADP-ribosyl)ation	49
	Non-Specific Proteolysis of DNA Polymerase β with Trypsin	50
	Co-Immunoprecipitation of PARP-1 Fragments with DNA Polymerase β	51
	Co-Immunoprecipitation of PARP-1 Apoptotic Peptide Fragments with DNA Polymerase β from Chromatin Extracts	51
IV.	Discussion	87
V.	Conclusions	98
	References	101

LIST OF ILLUSTRATIONS

Figure:	Page:
1. The Biochemical Pathways of Base Excision Repair	6
2. The Domain Structure of DNA Polymerase β	12
3. A 3-D Wire Representation of DNA Polymerase β	14
4. The Domain Structure of Poly(ADP-ribose) Polymerase-1	20
5. The Domain Structure of Caspase-3	25
6. The Comet Assay	56
7. The Design of a Selective EMSA probe for DNA Polymerase β	58
8. A Selective EMSA for DNA Polymerase β Binding	60
9. The Activity Gel Technique	62
10. DNA Polymerase β Activity Gels	64
11. Changes in DNA Polymerase β Activity as a Result of Covalent Poly(ADP-ribosyl)ation of PARP-1	66
12. DNA Polymerase β Activity Gels with Chromatin Extracts Following Covalent Poly(ADP-ribosyl)ation	68
13. Poly(ADP-ribosyl)ation of Chromatin Proteins	70
14. PARP-1 Activity Gels	72
15. Co-immunoprecipitation of PARP-1 with DNA Polymerase β	74
16. Proteolysis of PARP-1 with Caspases	76

17.	Proteolysis of PARP-1 with Caspases Following Poly(ADP-ribosyl)ation	78
18.	Proteolysis of PARP-1 in Chromatin Extracts with Caspases Following Poly(ADP-ribosyl)ation	80
19.	Non-Specific Proteolysis of DNA Polymerase β with Trypsin	82
20.	Co-immunoprecipitation of PARP-1 Apoptotic Peptide Fragments with DNA Polymerase β	84
21.	Co-immunoprecipitation of the PARP-1 Apoptotic Fragments with DNA Polymerase β from Chromatin Extracts	86
22.	Proposed model for PARP-1 as a switch between DNA repair and cell death	97
 Graph		
1.	Hela Cell Growth Curve	54

LIST OF ABBREVIATIONS

- β NAD⁺ - β -nicotinamide adenine dinucleotide
- AD - Automodification domain
- AP - Abasic, Apurinic/Apyrimidinic
- APE1 - Apurinic endonuclease 1
- BER - Base excision repair
- BRCT - Breast cancer gene C-terminus
- CD - Catalytic domain
- DBD - DNA binding domain
- dNTP - Deoxynucleotide triphosphate
- dRP - Deoxyribose phosphate
- EMSA - Electrophoretic mobility shift assay
- FEN1 - Flap endonuclease 1
- HhH - Helix-Hairpin-Helix
- MNNG - N-methyl-N'-nitro-N-nitrosoguanidine
- NLS - Nuclear localization signal
- OH - Hydroxyl
- pADPr - Poly adenosine diphosphate ribose
- PARP-1 - Poly(adenosine diphosphate ribose) polymerase-1
- PCNA - Proliferating cell nuclear antigen

PO₄ - Phosphate

Pol β - DNA polymerase β

XRCC1 - X-ray repair cross complimenting group factor 1

ZF - Zinc Finger

CHAPTER I

INTRODUCTION

Opening statement:

Eukaryotic cells are subject to insults that structurally damage the genetic material. Highly specialized pathways repair the DNA damage that involves chemical modification of bases [24]. One of these biochemical pathways is the mismatch repair system to correct improperly paired bases resulting during physiological DNA replication. Nucleotide excision repair corrects covalent base modifications that result in substantial structural irregularities within DNA. Conversely, repair of minor structural aberrations in DNA result from base excision repair (BER). This system is responsible for the repair of abasic (AP) sites. Interestingly, these AP sites are the most common form of DNA damage with an estimated frequency of 100,000 bases lost per cell per day [40]. Indeed, cells deficient in BER are highly inefficient at repairing abasic sites and are highly sensitive to alkylating and oxidative DNA damage. Excessive or unrepaired DNA damage by base alkylation or oxidation results in cell death. Therefore, a cellular requirement exists for a fully functional BER system and when impaired cell death predominates.

In this doctoral dissertation, a research project was developed to investigate some of the biochemical and molecular signals involved in regulating a switch between the opposing mechanisms DNA repair and cell death. Both are clearly required for protection against carcinogenesis [7]. However, a concise introduction to these highly sophisticated biochemical systems is provided first.

Base excision repair:

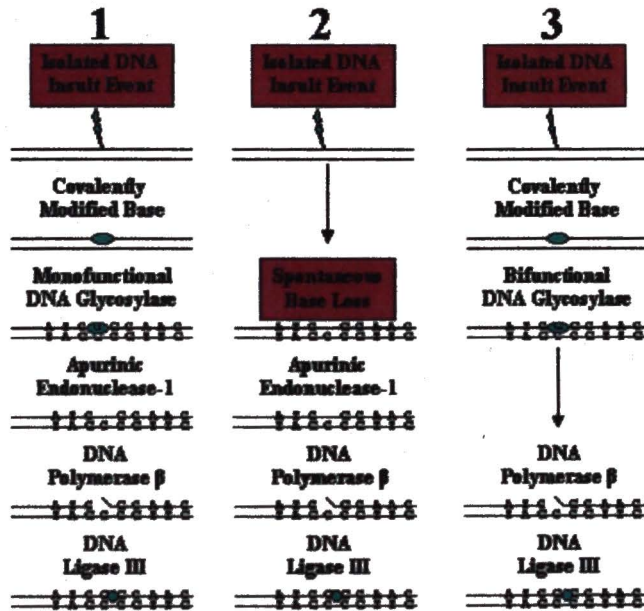
As expected, repair of DNA damage by the BER system involves a highly coordinated biochemical pathway. BER relies on multiple protein-protein interactions between several key DNA-metabolizing enzymes. This cascade of events may be visualized as a relay race with the runners (proteins) passing a baton (DNA), one to the next, without dropping it [80] (figure 1). Selection of the BER pathway is dependent on two variables: 1) the chemical nature of the DNA within the lesion site and 2) the enzyme initially recognizing the modified base. DNA glycosylases are first responsible for recognizing covalently modified bases [21]. DNA glycosylase recognition leads to the formation of an apurinic/apyrimidinic site by the hydrolysis of the N-C1 glycosidic bond between the modified base and the deoxyribose residue. Alternatively, spontaneous base loss can also lead to an apurinic or apyrimidinic site. The abasic site may then be processed by apurinic endonuclease 1 (APE1) [47]. APE1 catalyses a cleavage reaction that localizes 3' to the abasic site within the ribose-phosphate backbone. The result of these two initial reactions is the formation of a single strand break or lesion site. This lesion presents with both a 3'-hydroxyl (OH) and a 5'-deoxyribose phosphate (dRP) residue. DNA polymerases catalyze the transfer of a deoxynucleotide triphosphate (dNTP) to the terminal 3'-OH within the lesion in a template specific manner. The 5'-dRP residue is cleaved off to leave an intact 5'-phosphate group. DNA ligases are then responsible for rejoining the strands for completion of the BER pathway [77].

Single nucleotide repair, as presented, is the predominant BER pathway [58]. However, under distinct conditions, this repair system can also proceed via a long-patch

pathway. This occurs by either DNA glycosylase activity or the presence of alternate DNA chemistry within a lesion site. In contrast to single nucleotide BER, the long-patch repair pathway may result in the polymerization of 2-10 nucleotides [53]. This pathway requires the presence of the protein proliferating cell nuclear antigen (PCNA) [25]. Though PCNA is required for long-patch BER, both pathways demonstrate a strict dependence on the functional presence of DNA polymerase β (pol β) [EC 2.7.7.7] [57,58]. This unique polymerase is responsible for the synthesis of DNA within a lesion site by either of these two similar, yet distinct BER pathways.

Figure 1. The biochemical pathways of base excision repair. Two distinct pathways exist for BER and are classified as either single nucleotide or long-patch. Selection of repair pathway is dependent on either the chemical structure of the lesion site or the enzyme that initially recognizes the genetic damage. To provide further clarification, single nucleotide excision repair is presented as three separate pathways. From left to right they are: 1) Single nucleotide BER 2) Repair of an abasic site by single nucleotide BER and 3) Single nucleotide BER that involves a bifunctional DNA glycosylase.

1-Nucleotide Patch Pathways

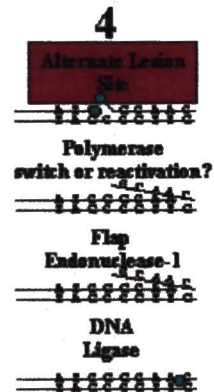


pol- β is Required for BER

Long Patch Pathway

PCNA Dependent

AP Site formed Pol. δ leading Ligase III leading



DNA polymerase β :

This enzyme is a key component of the mammalian enzymatic multi-protein complex responsible for repair of genetic lesions by BER. In fact, pol β is required for short patch and initiation of long patch DNA synthesis [57,58]. This enzyme is the smallest eukaryotic DNA polymerase containing 369 amino acids and is a modular protein with two primary peptide domains (figure 2). Each domain is independently associated with a specific catalytic function. A hypersensitive protease region of 14 amino acids connects these two domains [37]. Controlled digestion with a non-specific protease can be performed to separate these domains and has expedited the understanding of the role(s) this protein plays in DNA repair. Limited proteolysis by these techniques results in the generation of an 8 kDa N-terminal fragment that possesses a dRP lyase activity [42]. This peptide preferentially binds a 5'-dRP or a 5'-Phosphate (PO_4) group within DNA [59,60]. Further, this fragment preferentially binds single stranded DNA although it is capable of double stranded DNA binding [31]. However, and interesting to note, interaction with DNA is not sequence specific.

Techniques that utilize proteolytic digestion of pol β result in the generation of a unique 31 kDa C-terminal fragment. This peptide is capable of deoxynucleotidyltransferase activity [36]. In fact, the associated pol β deoxynucleotidyltransferase activity is completely contained within the 31 kDa fragment. This peptide does not possess significant DNA binding ability by itself in this form. Experiments that utilized additional protein degradation techniques indicate that the N-terminal proximal portion of the C-terminal fragment does however possess DNA

binding capability [11]. These results suggest that the DNA binding ability contained within the 31 kDa fragment and present within the intact protein can be masked. It is likely that a conformational change leads to such protein-DNA interactions.

With respect to intact pol β , the enzyme binds a lesion site as dictated by the 8 kDa domain. This interaction results from conformational changes that are lesion size dependent [30]. Differences in lesion size are accommodated by alternate pol β folding mechanisms. Conformational changes facilitated by the 8 kDa domain drive the correct placement of the C-terminal deoxynucleotidyl transferase domain.

As the smallest eukaryotic DNA polymerase, pol β has been crystallized and its three dimensional structure resolved [65,4]. In fact, crystal structures have also been resolved for pol β when bound to DNA substrates [55] (figure 3). Data of this nature indicate that the C-terminal 31 kDa domain is anatomically comparable to a "right hand". The palm region binds DNA with an interface that is not sequence specific yet selective for double stranded DNA. The thumb region forms half of a peptide loop that encircles the DNA at a point before the lesion site. The N-terminal domain is positioned off the fingers. To complete the formation of a peptide loop, this domain physically interacts with the thumb region of the 31 kDa domain. The trans domain interaction site is localized 5' to the DNA lesion. Both the N-terminal domain and the thumb region bind DNA through a helix-hairpin-helix (HhH) motif that is Mg^{+} dependent [54,56]. The binding of pol β to damaged DNA therefore results in a protein conformation that positions the 3'-OH moiety near the catalytic center of the 31 kDa domain. This

placement is primarily dependent on the HhH motif of the N-terminal 8 kDa domain yet is supported by the HhH motif in the thumb.

DNA polymerase β is active as a monomer and capable of a distributive deoxynucleotidyltransferase activity in the presence of single nucleotide gapped double stranded DNA. However, this polymerase can also synthesize DNA in a processive manner in the presence of DNA gaps formed by the absence of up to 6 nucleotides [67]. Indeed, the DNA involved in formation of the lesion site affects pol β activity. Interestingly, the presence of other polypeptides identified as components of the BER machinery can also effect changes in pol β activity. For example APE1 when bound to DNA, physically interacts with and stimulates the dRP lyase activity of pol β [5]. This activity of pol β is identified as the rate-determining step of most BER pathways [72]. Flap endonuclease 1 (FEN1) also functionally interacts with pol β and stimulates processive pol β activity and the generation of a flap structure by non-template 5' strand displacement. This flap structure is then recognized and further processed by FEN1 [61]. In addition, pol β may physically interact with either DNA ligase I or the X-ray cross complementing group factor 1 (XRCC1)/DNA Ligase III complex to facilitate the ligation step of BER [63,34,49]. It is likely that pol β remains bound to the lesion site and therefore remains unable to polymerize DNA within another lesion until this ligation occurs. Clearly multiple protein-protein interactions are involved in regulating pol β activity.

It has also been shown that pol β activity is attenuated in the presence of poly (adenosine diphosphate ribose) polymerase-1 (PARP-1) [EC 2.4.2.30] in a β -nicotinamide adenine dinucleotide (β NAD⁺) dependent manner [51]. Yet, in the absence of PARP-1 protein, pol β dependent BER is highly inefficient. PARP-1 is a highly abundant and constitutive chromatin protein enzymatically activated by DNA strand breaks and a component of the multi-protein BER complex [71,6].

Figure 2. The domain structure of DNA polymerase β . Pol β is a modular protein that is comprised of two distinct domains. The dRP lyase domain of the human pol β is 115 amino acids in length (8 kDa). The deoxynucleotidyltransferase domain is 240 amino acids long (31 kDa). A linker region of 14 amino acids joins these two domains. When this DNA polymerase is in a native form, the linker region is hypersensitive to proteolytic digestion.

**DNA Polymerase β :
369 Amino Acids**

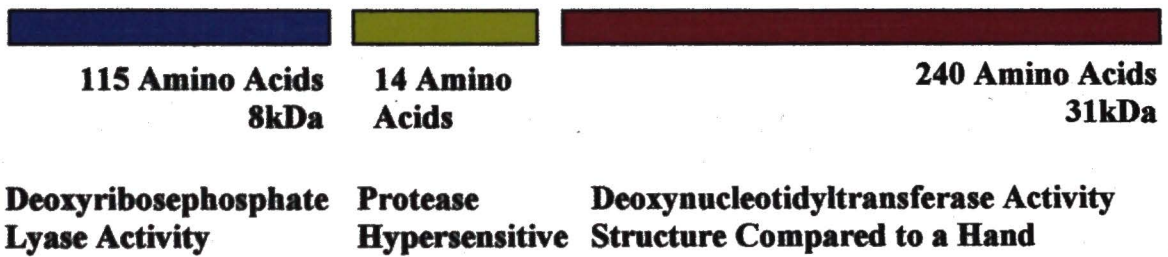
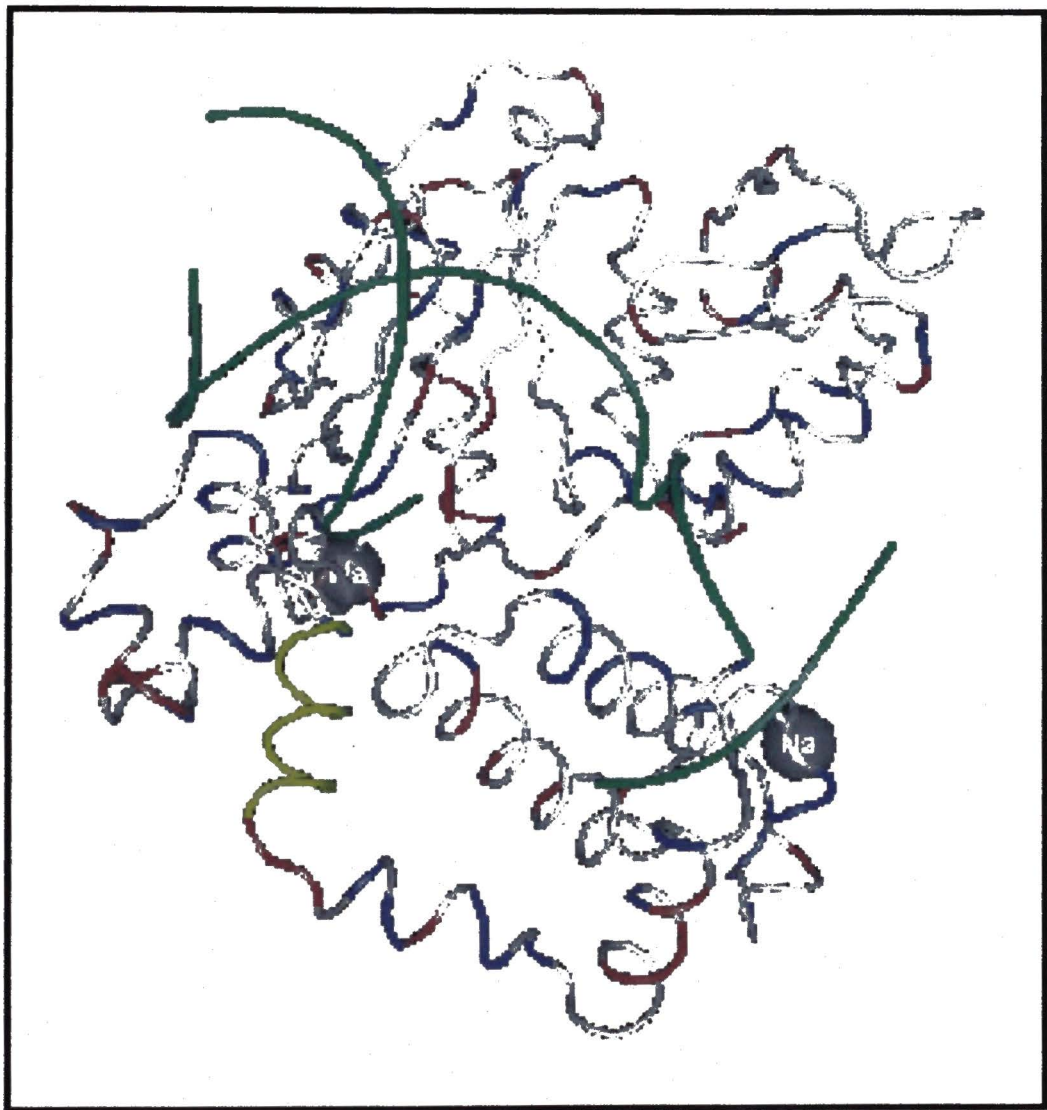


Figure 3. A 3-D wire representation of DNA polymerase β . A structural representation of pol β is presented in a complex with 5 nucleotide gapped double stranded DNA (Green) [55]. The positions of two Na^+ ions are also indicated (Grey). The linker region is highlighted in yellow at the lower left position of the protein structure. The deoxynucleotidyltransferase domain is on the top and the dRP lyase domain on the bottom right.



Poly (ADP-ribose) polymerase-1:

Poly adenosine diphosphate ribose (pADPr) was discovered in the lab of Paul Mandel in Strasburg France, over 40 years ago [12]. Later investigations into the synthesis of this nucleic acid lead to the discovery of the protein PARP-1 [9]. PARP-1 is the original member of a family of eukaryotic polymerases capable of synthesizing pADPr [48]. This specialized polymerase has been detected in all eukaryotic organisms with the notable exception of yeast cells. The expression levels of PARP-1 protein in the thymus, spleen, testes and brain are higher than other tissues [46]. PARP-1 localizes to the nucleus and is second in protein concentration only to histones. In fact, to provide an additional relation, PARP-1 molecules possess a stoichiometry of one molecule per every 1000 base pairs of DNA. Histones possess a stoichiometry of one molecule per 200 base pairs of DNA.

PARP-1 catalyzes the synthesis of pADPr with a strict dependence on the presence of DNA strand breaks. During this reaction, pADPr is chemically synthesized from the substrate βNAD^+ . Synthesized ADPr polymers are covalently bound to acceptor proteins, with PARP-1 itself serving as the primary acceptor molecule [10]. Therefore, PARP-1 bound pADPr is the result of automodification. Unlike most enzymes however, PARP-1 performs at least three distinct chemical reactions. PARP-1 initiates a chain of pADPr by the transfer of a single residue of ADPr to a glutamate residue within an acceptor protein. PARP-1 can also, by successive transfer of additional ADPr, elongate protein bound ADPr or pADPr to generate a linear homopolymer. PARP-1 catalytic activity may form polymers in excess of 200 residues in length with a branching

frequency of one every 40 ADPr residues. Therefore, PARP-1 can synthesize highly elongated and branched pADPr in the presence of DNA strand breaks.

Interestingly, the automodification reaction occurs via a catalytic homodimer. Thus, PARP-1 automodification takes place intermolecularly [44]. Further, heterodimerization can also affect protein-protein interactions of PARP-1 with other chromatin forming polypeptides [13].

Due to its nuclear abundance, PARP-1 has been suggested to be involved in multiple chromatin functions including DNA replication, transcription and DNA damage repair. The linear structure of PARP-1 and its unique subdomain structure lend itself to involvement in these chromosomal functions (figure 4). Though the native conformation of PARP-1 is globular, the linear structure indicates that it is a modular protein. PARP-1 can be separated into three distinct domains by proteolytic digestion. Each of these domains possesses a distinct function that is associated with the intact protein [33]. The N-terminal 46 kDa domain contains a DNA binding ability (DNA binding domain - DBD). Positioned within this domain are two zinc-finger (ZF) motifs and a bipartite nuclear localization signal (NLS). The two ZFs are involved in binding the enzyme to DNA strand breaks. The N-terminal proximal ZF (ZF1) is required for double strand breaks while the C-terminal proximal ZF (ZF2) is required for binding to single strand breaks [43,27]. Characterization of ZF motifs suggests that they are common to DNA binding proteins involved in non-sequence specific interactions. PARP-1 binding of nucleic acids is however not limited to DNA as it may bind mRNA under specific conditions [79].

The 54 kDa C-terminal domain of PARP-1 contains the catalytic activity associated with this enzyme (catalytic domain - CD). Within this region, a block of 50 amino acids comprises the established "PARP-1 signature". This signature peptide sequence is highly conserved between plants and animals and houses the β NAD⁺ binding site [78,41]. The CD, down to 40 kDa of the C-termini, is capable of a limited ADPr transferase activity in the presence of β NAD⁺ [66]. This activity is similar to the basal activity detectable from non-activated PARP-1.

The central 22 kDa domain or automodification domain (AD) of PARP-1 contains the initial ADPr acceptor sites. From this, at least four acceptor sites exist within the complete linear sequence of the protein and it is likely that the AD is covalently targeted first [45]. Interestingly, this domain also contains a Breast Cancer gene 1 C-terminus (BRCT) motif. This motif is identified as common to proteins involved in DNA damage repair [8].

A highly complex mechanism of PARP-1 protein-protein interactions is clear when considering that N-terminal DNA binding for C-terminal catalytic activation must be transduced through the AD. This suggests that protein-protein interactions of PARP-1 are likely to depend on the state of this molecule. This is important for several reasons. The first is that PARP-1 is a required component of the mammalian DNA BER complex [17,39]. Second, the bipartite NLS resides N-terminal to the AD and contains a proteolytic site that is recognized and cleaved during apoptotic cell death. This proteolytic event results in the physical separation of the DBD from the AD and CD and formation of two peptide fragments of 29 and 85 kDa. The separation of these domains

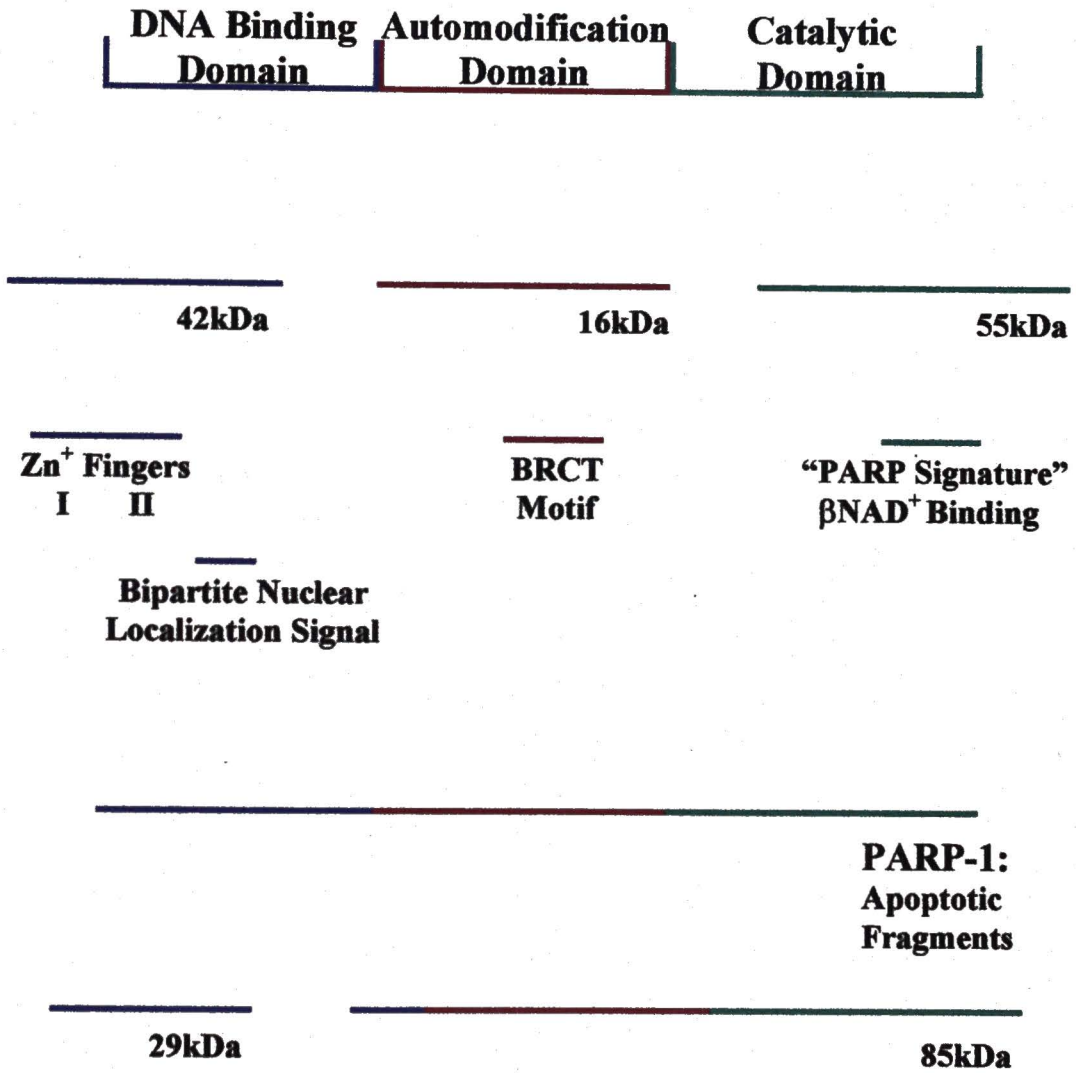
during apoptosis may lead to two novel and functional peptides that negatively affect BER and facilitate cell death.

In support, the 85 kDa fragment of PARP-1 is selectively removed from nucleoli during apoptosis while the 29 kDa fragment remains throughout the nucleoplasm [3]. Additionally, the resulting PARP-1 apoptotic fragments retain domain specific activity. The 85 kDa peptide selectively interact with DNA damage response related proteins [38]. In contrast, the N-terminal fragment demonstrates a high affinity for DNA strand breaks [70]. In fact, binding of the 29 kDa fragment to DNA ends serves as a competitive inhibitor of intact PARP-1 [16].

Due to the physiological significance of PARP-1 catabolism during cell death, a significant body of work has been generated to elucidate the cell biology of this event in DNA-damaged cells over the past few years. As presented below, two highly specific apoptotic proteases, that belong to a family of proteins called caspases, have been identified as the executioners of PARP-1 demolition.

Figure 4. The domain structure of poly(ADP-ribose) polymerase-1. The DNA binding domain is 42 kDa and N-terminal to the bipartite nuclear localization signal. Within this domain are two ZF structures required for DNA strand end binding. The AD (16 kDa) is central to the polymerase. This domain contains protein-protein interaction motifs and acceptor sites for ADP-ribose. The C-terminal 55 kDa of PARP-1 is the catalytic domain and contains the β NAD⁺ binding site within an established "PARP Signature". Proteolytic digestion of the intact polymerase by caspases generates two peptide fragments of 29 and 85 kDa from the N and C-termini respectively.

**PARP-1:
1014 Amino Acids**



Caspases:

At the molecular level, the execution phase of apoptosis is characterized by the proteolysis of key proteins, chromatin condensation and DNA fragmentation. These metabolic events of apoptosis require the activation of a group of proteins from a family of proteases called caspases [19]. Activation of these enzymes is required for the coordinated dismantling of the cell. A cellular presence of active caspases is in fact an indicator of apoptosis as they reside in zymogen forms in the cytoplasm of non-apoptotic cells. Activation from a proenzyme state is ultimately the result of a highly organized pathway. Caspases involved in this pathway are separable into two main groups depending on their hierarchical position. Initiator caspases are responsible for auto and heteroproteolysis of zymogens, e. g. caspase-9. Executioner caspases are responsible for effecting the initial cellular destruction associated with apoptosis. Together, caspase-3 [EC 3.4.22.-] and caspase-7 [EC 3.4.22.-] are considered the two primary executioners of apoptosis [67]. Both proteases are activated by caspase-9 [69]. Redundancy in substrate specificity is displayed by these executioner caspases and suggests the importance and complexity of a hierarchical proteolytic pathway of key cellular proteins [75,29,68]. Included in this redundancy is the proteolysis of the abundant nuclear enzyme PARP-1. Differences in the ability of these caspases to proteolyze PARP-1 may affect the progression of apoptosis.

The primary structure of human caspase-7 is 57% homologous to human caspase-3. In fact, it is 73% homologous with respect to amino acid composition and appears to differ by only 3 amino acid gaps (1%) (Blast Search). Each polypeptide possesses the

critical caspase signature with an amino acid sequence of QACRG that is identified as the domain responsible for substrate binding during proteolysis [20,32]. This peptide sequence possesses the required cysteine residue that caspases derive their name from (cysteine dependent aspartate specific proteases). Caspase-3 resides in the cytoplasm in a zymogen form as a 32 kDa protein and is processed into 16.6 and 12.9 kDa fragments during apoptosis to form the active protease [50]. Caspase-7 is 34.3 kDa in the zymogen form and also resides in the cytoplasm to be proteolytically activated into 19 and 13 kDa fragments [21]. Caspase-3 is active as a heterotetramer comprised of two copies of a heterodimer. The heterodimer is formed from one copy each of the two proteolytic fragments [64] (figure 5). Interestingly, this is believed to be the functional form of other caspases. The high level of homology between these executioners of apoptosis is supportive of their ability to proteolyze identical substrates. In support, the biochemical effects of pH, salt concentration and buffer composition are almost identical for the two caspases [73]. However, caspase-3 displays the greatest affinity for a protein substrate possessing a DQMD^tG sequence. By contrast, caspase-7 shows preferential affinity for a DQVD^tG sequence [75]. With regards to tissue expression, caspase-3 is detectable in all tissues and (-/-) mice are viable up to 1-3 weeks post-partum yet display abnormal development only in the brain [35]. Interestingly, the mRNA coding for Caspase-7 is not detectable in murine brain tissue [32]. Therefore, it appears that the function of each caspase may be tissue-specific with regards to cell death regulation.

From a mechanistic point of view in the presence of DNA, caspase-3 displays a reduced ability to proteolyze PARP-1 [15]. Following PARP-1 automodification in the

presence of low concentrations of βNAD^+ , Caspase-3 again displays a reduced proteolytic capability for PARP-1 [26]. Caspase-3 also possesses a slightly higher affinity over caspase-7 for the tetrapeptide DEVD. Though this sequence is recognized within PARP-1 by these caspases, this is only a limited observation of the enzyme-substrate interactions that are likely to result. Following DNA damage initiated apoptosis PARP-1 may not be present within the nucleus in a monomeric form. In contrast to caspase-3, caspase-7 possesses an affinity for protein free pADPr. Furthermore, caspase-7 is capable of proteolyzing PARP-1 automodified in the presence of 200 μM βNAD^+ [26]. Considering the fact that pADPr is a nucleic acid and similar to poly-adenylic single-stranded DNA it is likely that PARP-1 when present in chromatin is a substrate for caspase-7. In support, caspase-7 unlike caspase-3 possesses dense patches of lysine and arginine residues with 13.2% and 12.59%. Caspase-7 is likely the protease responsible for fragmentation of PARP-1 when present in active form. A careful analysis of the mechanistic aspects of the cellular degradation of PARP-1 is important to help clarify the cell death program under DNA damage conditions at the biochemical level.

Figure 5. The domain structure of caspase-3. This caspase is present in the cytoplasm in a zymogen form. The prodomain is initially cleaved off during proteolytic activation with the remaining peptide hydrolyzed into two proteins. A heterotetramer is formed by interactions between these two proteins to result in an active caspase molecule.

**Caspase-3:
341 Amino Acids**



**Cleaved and Not Part of the
Active Form of the Enzyme**



**Structure of the Active Form
of caspase-3**

Research prospectus:

The covalent modification of bases in DNA induced by either alkylation, oxidative stress or spontaneous base loss activates cellular DNA damage repair responses. As indicated previously, the primary DNA repair system responsible for correcting these prevalent genetic forms of damage is BER. An efficient cellular BER system requires the DNA repair polymerase pol β . This biochemical requirement is for the deoxynucleotidyl transferase activity associated with the enzyme. The absence of pol β in eukaryotic cells or extracts due to either gene knockout or immunodepletion results in a severely deficient BER system.

The DNA damage-dependent enzyme PARP-1 also appears to be essential for a competent BER system. Similar to pol β , the absence of this enzyme in extracts or intact cells also severely impairs the BER system. The biochemical reasons for this dependence are not completely understood at present. One possibility resides in the fact that PARP-1 is physically engaged in the BER complex. This physical participation by PARP-1 might provide for sensing of pivotal DNA intermediates formed during BER. Thus specific physical interactions between PARP-1 and other BER proteins sense and facilitate the progress of BER mediated by BER. As a mechanism to protect the integrity of the genome during BER, PARP-1 and pol β protein-protein, as well as protein-DNA interactions may provide a means to stabilize and facilitate multiple steps in the repair process and when repair is not progressing efficiently serve as a cellular switch to cell death.

Not surprisingly, these proposed roles for PARP-1 are under intense investigation worldwide with a wide variety of molecular and biochemical techniques are being employed. In most instances, the focus is placed on DNA damaged cells involved in a struggle for survival. In apoptotic cells however, a shift from survival to death by apoptosis coincides with PARP-1 proteolyzed into the apoptotic fragments of 29 and 85 kDa. This proteolysis results from caspase-3 and caspase-7 functioning synergistically to cleave and inactivate PARP-1 molecules. The resulting peptides are currently considered biochemical hallmarks of the execution phase of apoptosis. Therefore, in this research project, an experimental approach has been developed to investigate the molecular and biochemical interactions of PARP-1 and its apoptotic fragments with pol β in regard to the BER system.

Since the apoptotic fragments of PARP-1 retain domain specific activities, they are likely to, during execution of apoptosis, serve functional roles that facilitate cell death. For example, these roles would be reflected by a change in protein-protein interactions. Since PARP-1 physically interacts with pol β , association is expected to be retained during apoptosis, yet altered, due to the proteolysis of PARP-1 into peptide fragments. This interaction may also be a key factor to prevent unwanted DNA repair in the presence of fragmented chromatin that is generated during apoptotic cell death.

As shown below, this dissertation project describes experimental results that support the hypothesis that pol β non-covalently and specifically interacts with the physiologically relevant caspase generated peptide fragments of PARP-1. To accomplish this, PARP-1 fragments were first generated by proteolysis with either caspase-3 or

caspase-7. Both apoptotic enzymes displayed similar kinetics of proteolysis when using purified PARP-1 as a substrate, yet differences were observed when incubated with the active form of this polymerase. Results are also presented to demonstrate that both PARP-1 peptide fragments immunoprecipitate with pol β when using a reconstituted system or cell extracts, therefore suggesting that both apoptotic fragments physically and specifically interact with this DNA polymerase.

CHAPTER II

MATERIALS AND METHODS

Materials. Radiolabeled ^{32}P - βNAD^+ was obtained from ICN, Radiochemicals Division, Irvine, CA. Radiolabeled α - ^{32}P -TTP was obtained from PerkinElmer Life Sciences Inc., Boston, MA. Caspases were obtained from Pharmingen, San Diego, CA. DNA polymerase β was obtained from Trevigen, Gaithersburg, MD.

Purification of PARP-1. Recombinant Human PARP-1 protein was purified to homogeneity and was described in detail by Beneke et al., 2000 [5]. In short, Human PARP-1 cDNA was ligated into the baculoviral recombination plasmid pVL1393 (Pharmingen) and transfected into *Spodoptera frugiperda Sf9* cells by the instructions provided with the Baculogold kit (Pharmingen). Infection of *Sf9* cells was performed with a multiplicity of infection of 3 for production of recombinant protein. Purification of recombinant Human PARP-1 protein was carried out at 4°C during all steps. *Sf9* cells were lysed with protamine sulfate and proteins precipitated by first a 30 and then 70% ammonium sulfate cut. After 70% ammonium sulfate precipitation the pellet was dissolved in buffer B (100 mM Tris-HCl (pH 7.4), 10% glycerol, 0.5 mM EDTA, 12 mM β -mercaptoethanol and 1 mM PMSF). Sephadex columns were prepared by suspension of 1 g of Sephadex G-100-50 superfine (Sigma-Aldrich, St. Louis, MO) in buffer C [50 mM

Tris-HCl (pH 8.0), 1mM EDTA, 200 mM KCl, 1 mM DTT and 10 mM β -mercaptoethanol]. This suspension was loaded into a 60-mL glass syringe plugged with glass wool and washed once with 2 volumes of buffer D [50 mM Tris-HCl (pH 8.0), 0.5 mM EDTA, 5 mM MgCl₂, 5% glycerol, 12 mM β -mercaptoethanol and 1 mM PMSF]. Cell lysate samples were loaded on the column and eluted with 10 sample volumes of buffer D. Eluted PARP-1 protein was followed by western blotting and activity assays. Fractions containing the enzyme were pooled and used for oligo-dT/poly-A-cellulose column purification. These columns were loaded with 3 mL of eluted material, washed with 10 mL of buffer D, 2 mL of buffer D supplemented with 0.28 M KCl and 0.5 mL buffer D supplemented with 2.8 M KCl. Elution was performed by addition of 1.5 mL buffer D supplemented with 2.8 M KCl and immediately followed by the addition of glycerol to a final concentration of 20% (v/v). Samples were then applied to a Centriprep-50 cartridge (Amicon, Houston, TX) to concentrate the enzyme and then stored at -70°C. Purity was checked by 8% SDS-PAGE and followed by either Coomassie blue or silver staining.

Isolation of rat liver chromatin. Rat liver chromatin was isolated from freshly excised rodent tissue as described by Alvarez-Gonzalez, 1994 [2]. In short, rat livers were excised and washed with buffer A [10 mM Tris-HCl (pH 7.4) and 150 mM NaCl]. Minced tissue was homogenized in buffer B (12% (w/v) sucrose, 10 mM Tris-HCl (pH 7.8), 2.5 mM EDTA and 1 mM PMSF). The homogenate was filtered through cheese-cloth and centrifuged at 660xg for 5 min over 15% sucrose (w/v) in buffer C [10 mM Tris-HCl (pH 7.8), 10 mM NaCl and 1 mM PMSF]. Crude nuclear pellets were washed with 12%

sucrose (w/v) in buffer C, and then twice with 0.2% Triton X-100 (v/v) in buffer C, followed by pelleting over 15% sucrose (w/v) in buffer C. Pellets were further washed with 12% sucrose (w/v) in buffer C. Nuclei were resuspended in buffer C (pH 7.0) at a concentration of 1–6 mg of DNA/ml. Nuclei were placed on ice after the addition of EDTA (2.5 mM). The nuclei suspension was stirred gently for 15 min and then centrifuged at 12,000xg for 10 min. The supernatant was collected as chromatin.

Cell culture. Hela cells were maintained in 1500 mm² surface area dishes. Culture conditions involved incubation at 37°C in a humidified 5% CO₂ environment. Culture media was Dulbecco's minimal Eagle's medium (Sigma-Aldrich) that was supplemented with 10% fetal bovine serum (Sigma-Aldrich). Cells were supplied with fresh culture media every 24 hours. Cell harvesting was performed by removal of culture media followed by three successive washes in PBS solution [50 mM phosphate and 150 mM NaCl (pH 7.2)]. PBS was removed and adherent cells were proteolytically released by 10 min incubation in PBS solution that contained trypsin (Atlanta Biologicals Inc, Norcross, GA). Cells were pooled, gently centrifuged, then resuspended and washed three times in PBS. Cell proliferation was monitored by light microscopy where adherent cells were counted in 5 separate 1 mm² areas to provide means to calculate cell number. This was repeated at the designated times until 78 hours of culture was reached where by cells were harvested for further experimentation or for sub-culturing. Sub-culturing was performed with the seeding of 10,000 cells to each new culture dish

Comet assay. For this technique, Hela cells were incubated with N-Methyl-N'-nitro-N-nitrosoguanidine (MNNG) prior to subjection to the Comet assay. In short, cells were

either incubated with or without 100 μ M MNNG for 30 min while in culture. Cellular activity was halted by the removal of the MNNG containing solution and addition of ice-cold 10% trichloroacetic acid. Adherent cells were harvested by tryptic digestion as described previously then resuspended and washed three times in PBS. 1% low melting point agarose was added to the pellet to 1% (w/v) to resuspend cells. Immediately prior to use, microscope slides were dipped in a 1% normal melting point agarose (w/v) solution and allowed to dry followed by a second dipping. Once dry slides presenting with an even coat of agarose were selected. The agarose-cell solution was then painted onto these slides. Agarose painted slides were allowed to gel at 4°C for 1 hour. Following this period of time, cells on slides were lysed during a 1 hour incubation in lysis buffer [2.5 M NaCl, 10 mM Tris-HCl, 100 mM EDTA, 1% Triton X-100 (v/v) and 200 mM NaOH]. Slides were then placed in a vertical electrophoresis chamber and subjected to a constant voltage of 200 V for 1 hour. Following electrophoresis, slides were held for 1 hour in a sealed container filled with calcium sulfate. Slides were treated with the fluorescent dye SYBR green diluted 1:10,000. This dye was excited by exposure to light with a wavelength of 497 nm and visualized by confocal microscopy by filtering for emitted light at 520 nm.

Auto-poly(ADP-ribosylation) of PARP-1. PARP-1 was automodified under *in vitro* conditions by the catalytic transfer of the ADP-ribose moiety from β NAD⁺ while incubated in automodification buffer that contained activated calf thymus DNA. This reaction involved 5 min incubation at 37°C in automodification buffer [100 mM Tris-HCl (pH 7.8), 10 mM MgCl₂, 1 mM dithiothreitol and 20 μ g/mL of activated calf thymus

DNA (Sigma-Aldrich)] with the indicated concentration of βNAD^+ (radiolabeled ^{32}P - βNAD^+ where indicated). Additional reactions with caspases were performed where indicated. Following these incubations, proteins were separated by 10% SDS-PAGE. Wet gels were processed for Coomassie blue staining, silver staining or for the activity gel assay where indicated. When utilized, incorporation of radiolabeled substrate was visualized by autoradiography following the drying of gels.

Activity gels. Protein samples were electrophoresed by 10% SDS-PAGE polymerized in the presence of 50 $\mu\text{g}/\text{mL}$ of activated calf thymus DNA (Sigma-Aldrich). The gel slabs were washed four times for 15 min each at 37 °C with 100 mL of buffer A [10 mM Tris-HCl (pH 7.5) and 0.5 mM β -mercaptoethanol] to remove SDS. The gels were then incubated for 30 min at 37°C in 100 mL of buffer B [50 mM Tris-HCl (pH 7.5), 0.5 mM β -mercaptoethanol and 1 mM EDTA] supplemented with 5M guanidine HCl. Gels were then washed in 250 mL of buffer B four times for 1 hour each at 4°C. Next, the gels were pre-incubated for 1 hour at 4°C in 90 mL of DNA polymerization reaction buffer [70 mM Tris-HCl (pH 7.5), 7 mM MgCl_2 , 10 mM DTT and a mixture of the required deoxynucleotide triphosphates each at an initial concentration of 15 μM]. The DNA polymerase activity of pol β was assayed by incubation for 12 hours at 37°C in 10 mL of reaction buffer supplemented with 112 μCi of α - ^{32}P -dTTP as an activity tracer. The poly(ADP-ribosyl)ation activity of PARP-1 was assayed by incubation for 12 hours at 37°C in 10 mL of reaction buffer supplemented with 100 μCi of ^{32}P - βNAD^+ as the activity tracer. Reactions were terminated by incubation of gels for 1 hour at 37°C in 250

mL of 5% trichloroacetic acid supplemented with 100 μ M pyrophosphate tetrasodium. Gels were then washed seven additional times at 1 hour each at 37°C in the previously detailed TCA solution to reduce the presence of unincorporated substrates prior to drying. The *in situ* synthesis of nucleic acids was then visualized by the autoradiographic exposure of the dried gel.

Proteolytic Digestion of Proteins by Caspases. PARP-1 or chromatin extracts were subjected to sequence specific proteolysis by incubation with either Human caspase-3 or caspase-7 to generate apoptotic specific fragments of PARP-1. In these assays, substrate protein and either caspase-3 or caspase-7 were co-incubated at a 1:10 molar ratio (in extracts, PARP-1:caspase ratio was calculated with this polymerase assumed to be 1% of nuclear protein) for the indicated times in a protease buffer [20 mM PIPES (pH 7.2), 100 mM NaCl, 10 mM dithiothreitol, 1 mM EDTA, 0.1% CHAPS (w/v) and 10% sucrose (w/v)] at 37°C. Proteolytic reactions were terminated by boiling samples at 100°C for 5 min in Laemmli buffer. The generated peptide fragments were fractionated by 10% SDS-PAGE and were subsequently visualized by silver staining, Coomassie blue staining, autoradiography or further processed by activity gels where indicated. Percent proteolysis for each lane was calculated by taking densitometry readings of the 85 kDa bands and the respective control lane. The 85 kDa band readings were then normalized to controls.

Co-immunoprecipitation of PARP-1 peptides with DNA polymerase β . Where indicated, PARP-1 or chromatin extracts were first subjected to caspase-3 or caspase-7 proteolytic digestion as detailed above. Next, either the PARP-1 protein mixture or chromatin extracts were incubated with an equimolar amount of pol β for 30 min at 4°C in

immunoprecipitation binding buffer [10 mM Tris-HCl (pH 8.0), 150 mM NaCl and 0.1% Nonidet P-40 (v/v)]. Protein complexes were then incubated at 4°C for 1 hour with goat polyclonal anti-pol β antibodies (Santa Cruz Biotechnology Inc., Santa Cruz, CA). Immune complexes were subsequently incubated with protein-G agarose beads and then gentle rocking for 1 hour at 4°C. Protein complexes were sedimented by centrifugation at 12,000xg and resuspended three times in immunoprecipitation binding buffer. The supernatant was collected and pooled following each centrifugation step. Precipitates and supernatants were boiled at 100°C for 5 min prior to fractionation by 10% SDS-PAGE. Gels were then transferred to nitrocellulose membranes for western blotting.

Western blotting. Proteins were immobilized on nitrocellulose membranes and probed with either goat anti-PARP-1 or goat anti-pol β polyclonal antibodies and visualized by chemiluminescence. To accomplish this, membranes were incubated for 1 hour at 37°C in a blotting buffer [1 mM Tris-HCl (pH 8.0), 150 mM NaCl and 0.05% Tween-20 (v/v) with 5.0% non-fat milk (w/v)]. Where indicated, either anti-PARP-1 or anti-pol β antibodies (Santa Cruz Biotechnology Inc.) were added with a final dilution of 1:1000 followed by 1 hour incubations at 37°C. Membranes were then washed three times in blotting buffer for 10 minutes at 37°C. Finally, membranes were incubated for 1 hour at 37°C with mouse derived anti-Goat IgG secondary antibodies conjugated to horse-radish peroxidase (Sigma-Aldrich). Secondary antibodies were diluted 1:1000 in blotting solution. Nitrocellulose bound protein-antibody complexes were visualized by enhanced chemiluminescence as suggested in the ECL Plus chemiluminescence kit obtained from Amersham Pharmacia, Piscataway, NJ.

Electrophoretic mobility shift assay. A probe for pol β was designed with each single stranded DNA molecule synthesized by Integrated DNA Technologies, Coralville, IA. The 5' end of the primer strand (P1) was selectively radioactively labeled. To achieve this, P1 was annealed to the template strand (Tm) by combining equimolar amounts of each in annealing buffer [250 mM KCl and 50 mM Tris-HCl (pH 8.0)]. This mixture was heated to 65°C and then incubated for 10 min in a sequential manner in water baths of the following temperatures: 65, 37, 22 and 0°C. The resulting complexes were incubated with T4 DNA polynucleotide kinase (United States Biochemical Corp., Cleveland, OH) in the presence of [γ -³²P]ATP in kinase buffer [50 mM Tris-HCl (pH 7.5), 10 mM MgCl₂ and 10 mM β -mercaptoethanol] for 30 min at 37°C. This mixture was heated to 95°C for 5 min. The non-primer strand (P2) was added at this point equimolar to P1 and Tm. As before, the DNA samples were sequentially transitioned from 65 to 0°C to permit annealing. The primary structure upon annealing of single stranded DNA molecules is presented in figure 7. Once generated, 10 ng of the probe was incubated with purified pol β or chromatin extracts for 30 min in binding buffer [20 mM Tris-HCl (pH 8.0), 60 mM KCl, 5 mM MgCl₂, 1 mM dithiothreitol, 0.05% Nonidet P-40 (v/v) and 10% glycerol (v/v)] for 20 min at 27°C. These samples were electrophoresed at 4°C in a 5% polyacrylamide gel that contained 17.8 mM tris-borate and 0.4 mM EDTA. The gel was then dried and visualized by autoradiography.

Tryptic digestion of DNA polymerase β . Pure pol β protein was incubated with trypsin (Atlanta Biologicals Inc.) to generate peptide fragments of this DNA polymerase. Incubations were in digestion buffer [25 mM Tris-HCl (pH 7.5), 25 mM NaCl and 1 mM

EDTA]. Substrate to enzyme ratios were as indicated with incubations for 1 hour at 24°C. Boiling samples in Laemmli buffer terminated the proteolytic reactions. Resulting peptides were separated by 15% SDS-PAGE and then stained with Coomassie blue. Gels were then dried.

CHAPTER III

RESULTS

The Comet assay

An initial objective of this project was to establish a routine assay that would allow for the quantification of pol β mediated DNA synthesis. For this, the Comet assay was employed. This procedure permits sampling of individual cells and is ideal to quantify the density of DNA excision sites per the cell genome [76]. Subjecting cells to the Comet assay results in migration of DNA and formation of an image similar to a 'comet' when the genetic material is fluorescently labeled and visualized. DNA fragment migration can then be correlated to the extent of genotoxic insults incurred by the cell with increased fragmentation resulting in increased migration. This technique is also called single cell gel electrophoresis.

Human cervical cancer cells were selected for the Comet assay. Cells were cultured until logarithmic growth and then harvested for counting [28]. Results of growth curves were graphed as cell number on the y-axis and time of culture on the x-axis (graph 1). The number of cells counted for each time point was averaged and standard deviations calculated. By determining the point of intersection for the midpoint in logarithmic growth with the x-axis, a time was established for harvesting of cells. As indicated by the

blue vertical line in graph 1, 78 hours of culture was repeatedly used to provide similar harvesting conditions.

Cultured Hela cells were subjected to DNA damage by incubation with N-methyl-N'-nitro-N-nitrosoguanidine (MNNG). Following MNNG treatment, cells were prepared for the Comet assay as described previously. In figure 6A, a representative image of an untreated cell is shown. The electrophoretic migration of DNA was indicated by a fluorescence signal within the boundary of the membrane. However, this migration was minimal when compared to MNNG treated cells. Figure 6B is a representative image of cells treated with 100 μ M MNNG for 30 min. The migration distance of DNA from these cells was noticeably greater than untreated cells. The difference in fluorescence intensities was attributed to an increase in DNA strand breaks since fluorescent labeling was specific for DNA strand ends.

The Comet assay permits detection of both single and double strand breaks formed during DNA repair metabolism and is therefore highly suited for break detection following cellular exposure to DNA damaging agents. Repair activity was, however, recently determined to not be exclusive to pol β or the BER system. As an example, DNA strand breaks may form as a result of other nuclear functions, *ie* topoisomerase activity. The Comet assay was abandoned for these reasons to establish biochemical assays specific for pol β activity.

Experimental design to generate a DNA substrate for DNA polymerase β binding

DNA polymerase β recognizes specific DNA intermediates formed during BER metabolism. The design of a molecule specific for pol β binding involved the independent synthesis of three distinct DNA fragments. A template strand was identified as Tm. It consisted of 27 nucleotides of poly-deoxyadenosine and was bordered on both ends by a single deoxyguanosine. A primer strand was labeled P1. It possessed a free 3'-OH group required for pol β deoxynucleotidyltransferase activity. P1 also consisted of 11 bases of poly-deoxythymidine and was bordered on the 5' end by a single deoxycytidine. The third strand was labeled P2 and consisted of 11 bases of deoxythymidine. It was bordered by a single deoxycytidine on the 3' end. P2 also possessed a single phosphate moiety on the 5' end. Upon annealing of both the P1 and P2 oligos to Tm, a primary product was formed that was double stranded and 27 bases in length. This molecule possessed a 5-nucleotide gap between the P1 and P2 strands. Thus, the gap of this engineered DNA molecule was bordered by a 3'-OH and a 5'-P(O₄). The structure of this pol β substrate is presented in figure 7.

Electrophoretic mobility shift assays specific for DNA polymerase β

Highly purified human recombinant pol β was subjected to electrophoretic mobility shift assays (EMSA) using the probe described previously. The DNA duplex was first radioactively labeled with T4 polynucleotide kinase as detailed previously. Pure pol β was subsequently incubated with an excess of probe in annealing buffer. The

sample was then electrophoresed under non-denaturing conditions to monitor the protein-DNA complexes formed. Gels were then dried and subjected to autoradiography.

As indicated by results presented in lane 1 of figure 8, unbound probe electrophoresed to the bottom of the gel. In lane 2, we observed the presence of a single band at the top of the gel indicating that pol β efficiently bound the probe. To address binding specificity, an additional incubation was performed. Rat liver chromatin extract was incubated with radiolabeled probe instead of purified pol β protein. Figure 8, lane 3 presents results to suggest that no more than two different protein-DNA complexes form following incubation of chromatin extracts with this DNA duplex. Unbound probe was again detected at the bottom of the gel. The gel-shift nearest the bottom of the gel in lane 3 is an unidentified complex at this time. In addition, another shift was detected at the top and positioned similar to the shift formed by the binding of pure pol β protein to radiolabeled probe.

Additional experiments were also performed to address the effects of PARP-1 automodification on the formation of pol β -DNA complexes using this technique. This involved a prior incubation of chromatin extracts with β NAD⁺ to generate poly(ADP-ribosyl)ated proteins. The molecules generated were then incubated with pol β and radiolabeled DNA substrate then subjected to EMSA. The results from these experiments were not however conclusive enough to indicate a change in pol β affinity for this molecule. Apparently, in the presence of polymer free and ADP-ribosylated proteins an electrophoretic smear resulted. Though demonstrating an ability to utilize pol β by

EMSA, this technique was not used further due to absence of clear results generated in the presence of activated PARP-1.

DNA polymerase β specific activity gel assay

As an alternate experimental approach to determine if pol β is regulated by PARP-1, we subjected this DNA polymerase to PARP-1 poly(ADP-ribosyl)ation conditions and then assayed for pol β activity. This was achieved using pol β specific activity gels prepared with activated calf thymus DNA. A representative flow chart of the technique is presented as figure 9. Purified pol β protein was assayed for DNA synthesis by activity gel initially. To test for enzymatically active pol β molecules by *in situ* DNA synthesis, gels were incubated in activity buffer containing radiolabeled deoxythymidine triphosphate. Unincorporated nucleotides were washed from the gel prior to drying. Dried gels were then subjected to autoradiography.

Panel 10A, lane 1 are pure pol β and PARP-1 proteins separated by 10% SDS-PAGE followed by Coomassie blue staining. In addition, lane 2 are electrophoretically separated chromatin proteins also Coomassie blue stained. These lanes were excised prior to the activity gel assay. The results demonstrate the banding patterns formed by electrophoresis of pure and chromatin proteins as well as the abundance of polypeptides within the chromatin extracts. From the results presented in figure 10B, a single band was detected when pure pol β protein was assayed by DNA polymerase activity gels. This experiment was then repeated with rat liver chromatin extracts even though multiple DNA polymerases are known to be present in these crude isolates. The results shown in

figure 10C indicate that a single band was observed and corresponded to the established electrophoretic position of pure pol β indicating that this technique is selective for DNA synthesis by this polymerase .

DNA polymerase β activity gels following protein-poly(ADP-ribosyl)ation

Next, the question of whether PARP-1 mediated poly(ADP-ribosyl)ation regulates pol β activity was addressed. Experiments described below only addressed the deoxynucleotidyltransferase activity of pol β . Protocols were repeated as described previously following with an additional incubation. Prior to electrophoresis, either pol β or chromatin extracts were incubated under poly(ADP-ribosyl)ation conditions at the specified β NAD⁺ substrate concentrations. The results presented in figure 11, lane 1 indicated the expected position of pure pol β within the activity gel. DNA polymerase β was incubated in automodification buffer in the absence of PARP-1 prior to assaying by activity gel. Figure 11, lane 2 shows that no detectable change results when compared to the control lane (lane 1). We then subjected pol β protein to PARP-1 automodification conditions prior to activity gels. Results presented in figure 11, lanes 3 and 4 indicated that under these conditions pol β activity was independent of the β NAD⁺ concentration used for protein-poly(ADP-ribosyl)ation.

DNA polymerase β activity gels with chromatin extracts following covalent poly(ADP-ribose)ation

In addition to results presented in figure 11, experiments were performed with chromatin extracts. DNA polymerase β and PARP-1 were indicated to be present within these extracts (PARP-1 results presented in figure 14). Initially, chromatin extracts were incubated in the presence of enzymatic buffer components prior to electrophoresis and the activity gel procedure. The results from this experiment provided a control activity level and expected electrophoretic position of pol β when using rat liver chromatin proteins (figure 12, lane 1). Additionally, chromatin extracts were incubated under poly(ADP-ribose)ation conditions with the indicated concentration of radiolabeled β NAD⁺ prior to the activity gel procedure. The results presented in figure 12, lane 2 indicated that detected pol β activity is comparable to the control lane.

Poly(ADP-ribose)ation of chromatin proteins

To demonstrate that protein-poly(ADP-ribose)ation takes place in chromatin extracts, samples were subjected to poly(ADP-ribose)ation conditions at the indicated β NAD⁺ concentrations. The addition of radiolabeled β NAD⁺ facilitated the identification of poly(ADP-ribose)ated proteins. Panel 13A, lanes 1 and 2 are chromatin proteins separated by 10% SDS-PAGE and Coomassie blue stained following incubation with β NAD⁺ at the indicated concentrations. Panel 13B, lanes 1 and 2 are autoradiogram results of the same gel presented in panel 13A. Present within panel 13B, lane 1 are

radiolabeled ADP-ribosylated proteins with molecular masses of 114, 85, 65, 50, 40, 32, 29, and <15 kDa. An absence of migration for these proteins was observed when the concentration of βNAD^+ was increased from 0.20 to 100 μM (lane 2).

PARP-1 activity gel assay

Specific activity gels were also performed for PARP-1. These experiments were carried out to generate additional results with this technique when using a polymerase that is also a substrate for ADP-ribose polymers. Initially, highly purified human recombinant PARP-1 was assayed for *in situ* enzymatic activity. Pure protein was electrophoresed under denaturing conditions utilizing a polyacrylamide gel that was polymerized in the presence of nicked calf thymus DNA. Activity from renatured proteins was assayed by incubating gels in an activity buffer that contained radiolabeled βNAD^+ . Gels were dried and autoradiographed to detect PARP-1 activity.

Results presented in figure 14A, lane 1 demonstrate that enzymatic activity of renatured PARP-1 was detectable *in situ*. A single radioactive band was formed at an expected 114 kDa electrophoretic position. To determine if this assay was selective for PARP-1, we repeated the experiment with rat liver chromatin extracts. PARP-1 was detected using identical activity gel assay conditions as mentioned above (14A, lane 2). This was apparent by the presence of a single band of 114 kDa that co-localized to a position identical to pure PARP-1 (lane 1). Also, no alternate bands were detected in lane 2.

Next, chromatin extracts were subjected to protein-poly(ADP-ribosyl)ation prior to assaying by activity gels. This involved an additional incubation of chromatin protein with the indicated concentrations of βNAD^+ under poly(ADP-ribosyl)ation conditions. As presented in panel 14C, the results demonstrate that no detectable change in activity occurred when comparing the control lane (lane 1) and the experimental (lane 2).

Co-immunoprecipitation of PARP-1 with DNA polymerase β

Physical interaction between pol β and PARP-1 was also investigated since the former is a substrate for the covalent addition of ADP-ribose polymers. To examine if molecular interactions between these two polypeptides are sufficient for co-immunoprecipitation to occur, highly purified human recombinant PARP-1 and pol β were added at equimolar quantities in binding buffer. Immunoprecipitation reactions were performed as presented previously. Proteins immobilized on nitrocellulose were probed for the presence of either pol β or PARP-1. DNA polymerase β western blotting involved polyclonal antibodies that recognize the N-terminal 20 amino acids of this protein. Probing for PARP-1 was performed with polyclonal antibodies that recognize a 20 amino acid N-terminal fragment of this protein. Bound antibodies were detected by chemiluminescence using secondary polyclonal antibodies conjugated to horse-radish peroxidase.

The results presented in figure 15A show that pol β was able to be immunoprecipitated then detected by western blotting. Western blotting with anti-PARP-1 antibodies indicated that this protein was also present in the precipitated material (15B).

Proteolysis of PARP-1 with caspases

The proteolysis of PARP-1 with caspases was investigated with the intent of establishing a procedure to generate the specific apoptotic peptide fragments of this polymerase. To accomplish this, the executioner caspases 3 and 7 were co-incubated with pure PARP-1 protein. Incubations were carried out in caspase proteolysis buffer. The protein substrate was added in solution with a 10-fold molar excess to either caspase-3 or caspase-7 as the enzyme. The time of incubations for proteolysis are indicated on the legend (figure 16). Resulting peptides were then electrophoresed under denaturing conditions and the gels were stained with silver.

The results presented in figure 16A indicated that the kinetics of PARP-1 proteolysis by caspase-3 were complete within 30 minutes. This degradation generated the two expected PARP-1 fragments with the 85 kDa peptide shown. Continuation of this incubation for 240 minutes did not result in additional proteolysis of PARP-1. As a control, 80 ng of intact PARP-1 was electrophoresed in lane 1. Comparing the band intensities in lanes 2-4, where 200 ng of PARP-1 was utilized, we estimated that greater than 80% of the caspase substrate was degraded. When comparing these results to experiments that involved caspase-7, minor differences were observed. Although the

kinetics of proteolysis were similar, less product was formed by use of caspase-7. Again, comparing band intensities, product to the control lane, we estimated that greater than 50% of PARP-1 was converted into the apoptotic fragments. To provide a semi-quantitative analysis of proteolytic efficiency for each caspase, densitometric readings were obtained for each time point and controls. Readings obtained from times of proteolysis were normalized against the control lanes to permit calculation of percent proteolysis. Values are therefore provided as the percent proteolysis at each time and presented in figure 16.

Proteolysis of PARP-1 with caspase-3 following poly(ADP-ribosyl)ation

Next, experiments were performed to address whether caspase-3 can proteolyze poly(ADP-ribosyl)ated PARP-1. For these experiments, the polymerase was subjected to automodification conditions prior to incubation with caspase-3. PARP-1 poly(ADP-ribosyl)ation was carried out at the indicated βNAD^+ concentrations. Gels were stained with Coomassie blue to visualize only the peptide species. The results presented in figure 17 show that, as the concentration of βNAD^+ was increased, proteolysis of PARP-1 was less detectable. A PARP-1 control (lane 1) was electrophoresed without prior incubation with caspase-3. In addition, nonmodified PARP-1 was efficiently proteolyzed by caspase-3 as shown in the control in lane 2. Lanes 3 and 4 show results that as the βNAD^+ concentration was increased, the presence of PARP-1 fragments decreased. However, as previously demonstrated, protein-poly(ADP-ribosyl)ation with 100 μM

βNAD^+ results in a loss of electrophoretic migration for modified species. The absence of bands in lane 4 may then be attributed to proteins remaining at the origin of the gel.

Proteolysis of chromatin proteins with caspases following protein-poly(ADP-ribose)ation

To further investigate if either caspase-3 or caspase-7 proteolyze PARP-1, additional experiments were carried out using a reconstituted chromatin environment. Chromatin extracts were subjected to poly(ADP-ribose)ation in the presence of radiolabeled βNAD^+ prior to the addition of either exogenous caspase-3 or caspase-7. Poly(ADP-ribose)ation conditions were performed with the indicated concentrations of βNAD^+ . The resulting samples were electrophoresed under denaturing conditions. Gels were then dried, stained with Coomassie blue and subjected to autoradiography.

The results presented in figure 18A, lane 1 show chromatin proteins incubated with 0.20 μM βNAD^+ and are presented as a control. Lanes 2-4 of figure 18A are results from experiments performed with chromatin proteins following poly(ADP-ribose)ation with increasing concentrations of βNAD^+ as indicated. Co-incubation of caspase-3 with chromatin extracts did not result in detectable proteolysis of PARP-1. These experiments were repeated with caspase-7 and presented as figure 18B. The results in figure 18B, lane 1 indicated that caspase-7 co-incubation results in detectable proteolysis of poly(ADP-ribose)ated PARP-1. However, as the βNAD^+ concentration was increased (compare 18A, lanes 3 and 4 to 18B, lanes 2 and 3), co-incubation with caspase-7 did not result in,

the detectable presence of proteolysis of modified PARP-1 molecules as was presented for caspase-3. At these βNAD^+ concentrations, radiolabeled proteins smeared within each lane or remained at the origin of the gel. Coomassie staining of gels did not however indicate that proteins were smeared within each lane at these higher βNAD^+ concentrations. In addition, these results provided an internal control to ensure loading of equal amounts of protein for each lane. Therefore, bands formed by histone H1 are provided as figures 18C and D.

Non-specific proteolysis of DNA polymerase β with trypsin

Next, we wanted to perform experiments to determine if pol β could be proteolyzed into domain specific peptide fragments to be used for additional experiments addressing interaction between this polymerase and PARP-1. These experiments however utilized the non-specific protease trypsin and therefore generated non-physiological fragments of pol β . DNA polymerase β protein was incubated with trypsin for 30 minutes over a range of enzyme:substrate ratios. Peptide fragments generated were electrophoresed under denaturing conditions by 10% SDS-PAGE. These gels were then stained with Coomassie blue.

Results of proteolytic digestions are presented in figure 19. Lane 2 shows a tryptic digestion of pol β with a ratio of 1:1000 that did not result in detectable peptide fragment generation. However, proteolysis of this protein substrate with a ratio of 1:10 did result in two primary products with molecular weights of 31 and 8 kDa. These results are

presented in figure 19 lane 3. The molecular weights for the top and bottom bands correlated with the established molecular weights of the C and N-terminal domains of pol β respectively. Alternate bands were detected when proteolysis of pol β was performed with the molar ratio of 1:10. These bands are visible in lane 3 at 27 and 22 kDa. Due to the presence of alternate peptides following trypsin digestion, we determined that this technique was not sufficient for peptide interaction studies yet did support previously published data relative to the domain structure of this polymerase.

Co-immunoprecipitation of PARP-1 apoptotic fragments with DNA polymerase β

To investigate if PARP-1 apoptotic fragments interact with pol β *in situ*, co-immunoprecipitation experiments were performed. These experiments were identical to those conducted with intact proteins, except that pure PARP-1 was subjected to caspase-3 proteolysis for 1 hour prior to immunoprecipitation. Caspase-3 was selected to proteolyze PARP-1 following results generated with pure components and presented in figure 16.

The results presented in figure 20A and B indicated that each PARP-1 apoptotic fragment was detectable in the immunoprecipitated material. As a negative control, immunoprecipitation was also carried out in the absence of anti-pol β antibodies (lane 1). Collected supernatant material was electrophoresed and is presented as results in lane 2. Lane 3 are the results from the co-immunoprecipitation experiment as presented above.

Co-immunoprecipitation of PARP-1 apoptotic peptide fragments with DNA polymerase β from chromatin extracts

To further examine if the apoptotic fragments of PARP-1 physically interact with pol β *in situ*, co-immunoprecipitation experiments were conducted with chromatin extracts. No exogenous PARP-1 or pol β proteins were therefore added. To perform these experiments, we first subjected chromatin extracts to caspase-7 proteolysis. This protease was selected based off of results presented in figure 18.

The results presented in figure 21A and B suggested that PARP-1 apoptotic peptide fragments were immunoprecipitated with pol β . Lanes 1 and 2 are results carried out in the absence of anti-pol β antibodies. From these control experiments, neither PARP-1 fragment was observed in the precipitated material (panel A & B, lane 1). However, the 85 kDa fragment was observed in the supernatant as presented in panel A & B, lane 2. When this experiment was performed as mentioned above and in the presence of anti-pol β antibodies, each PARP-1 polypeptide was detected in the precipitated material (panel A and B, lane 3). Only the 85 kDa PARP-1 fragment was detected in the supernatant material (lane 4).

Graph 1. Hela cell growth curve. Cells were plated, grown and counted at the indicated times. The growth curve was generated from repeated cell counts at the indicated times to provide a means to establish a midpoint in logarithmic growth. The period of 78 hours was used as the exact time of culture for cells prior to harvesting.

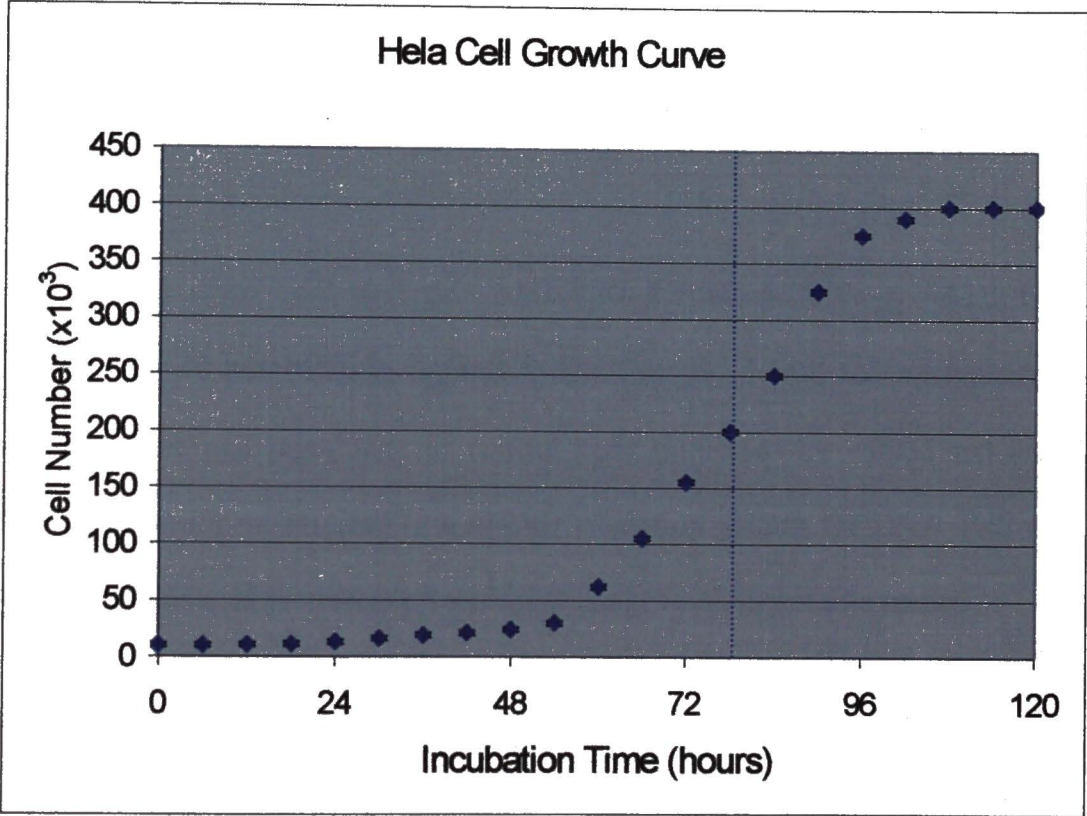
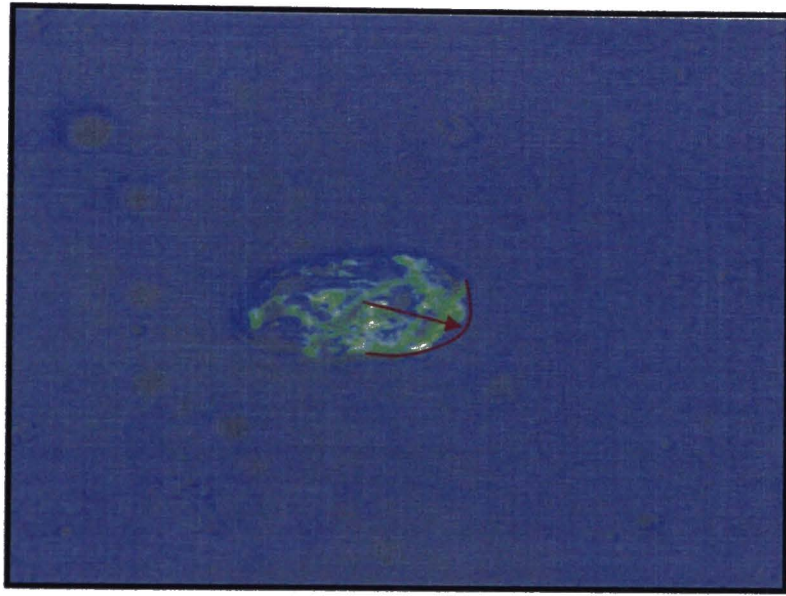


Figure 6. The Comet assay. Cells were assayed following treatment without (6A) or with 100 μ M MNNG for 30 min (6B). In figure 6A, DNA migrated with an electrophoretic front just beyond the cell membrane of control cells (indicated by curved red line). However, MNNG treatment resulted in a distinct migration pattern for DNA such that labeling of this nucleic acid produced a fluorescent image reminiscent of a comet.

A



B

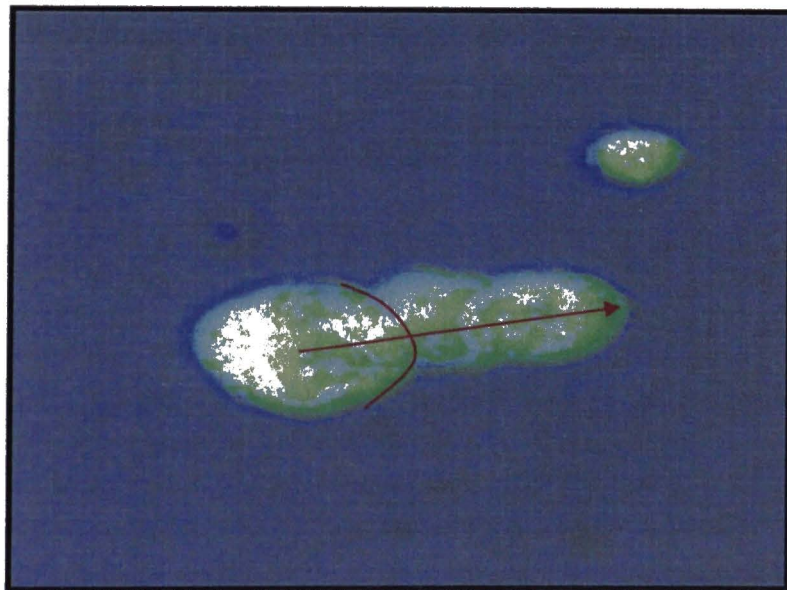


Figure 7. A selective EMSA probe for DNA polymerase β binding. A DNA duplex with a five nucleotide gap was produced to investigate specific binding to pol β . A poly-A template strand (T_m) was 3' and 5' capped with G to coordinate primer strand (P1) and non-primer strand (P2) annealing. The P2 strand contained a 5'-P(O₄) group to facilitate pol β binding. The DNA probe was radiolabeled only at the 5' end of the P1 strand with T4 polynucleotide kinase as indicated in the materials and methods section.

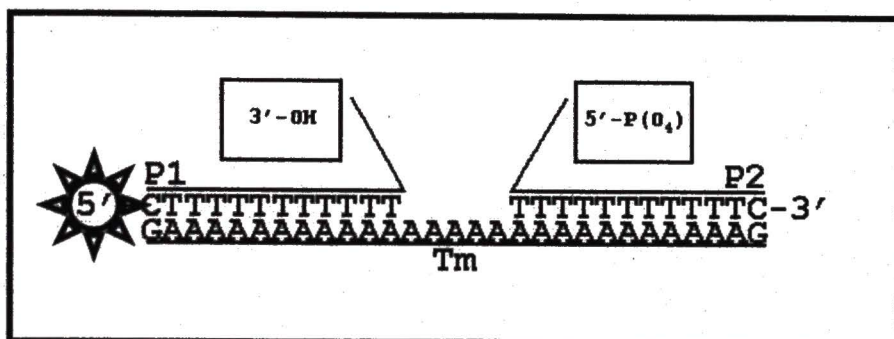


Figure 8. A selective EMSA for DNA polymerase β binding. Pure radiolabeled DNA probe (figure 7) was electrophoresed in a 5% non-denaturing gel (lane 1). Pure pol β protein was incubated with this radiolabeled substrate for 30 min at 27°C and then subjected to non-denaturing electrophoresis (lane 2). Rat liver chromatin extracts were also incubated with the probe and electrophoresed into a 5% non-denaturing gel (lane 3).

Chromatin			+
Pol β		+	
DNA Probe	+	+	+

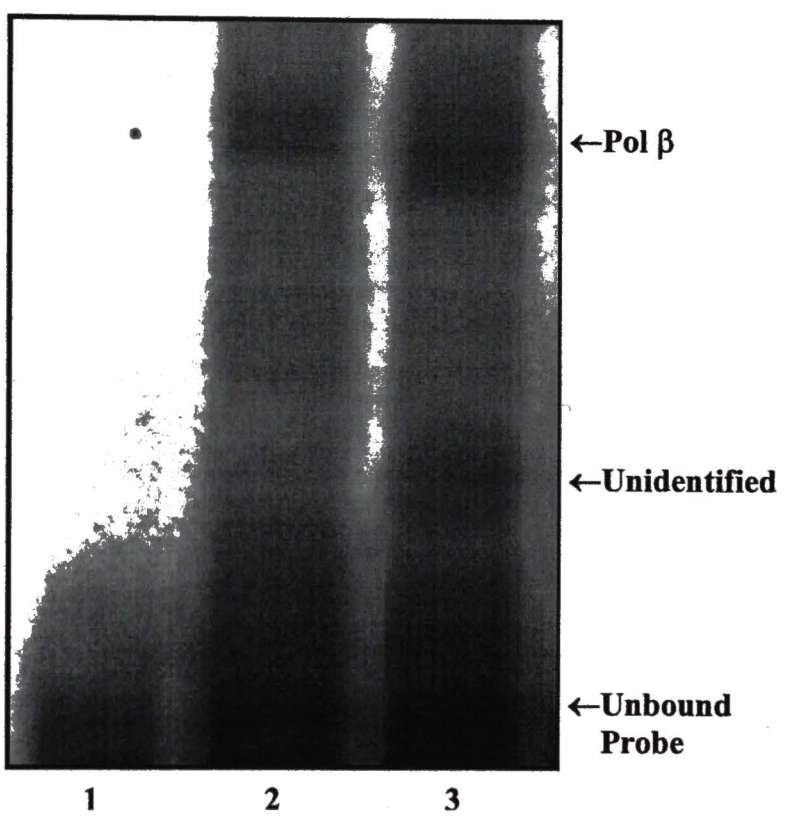


Figure 9. The activity gel technique.

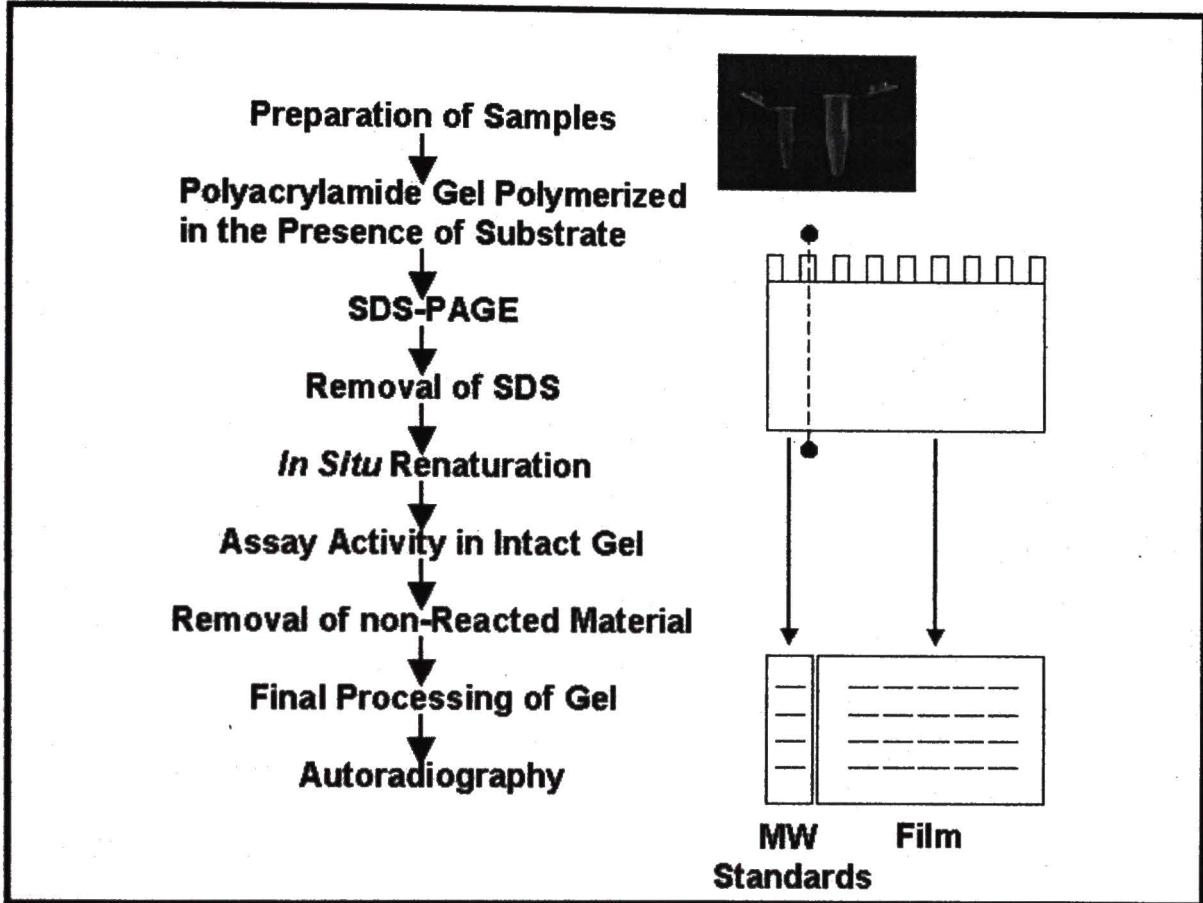


Figure 10. DNA polymerase β activity gels. Pure pol β and PARP-1 were separated by 10% SDS-PAGE and Coomassie blue stained (panel A, lane 1). Chromatin proteins were also electrophoresed and stained under identical conditions (lane 2). Pure pol β was subjected to the activity gel technique. In 10B, pol β was electrophoresed by 10% SDS-PAGE and assayed by activity gel. In panel 10C, extracted chromatin proteins were also subjected to the activity gel technique following separation by 10% SDS-PAGE.

Pol β	+	-	+	-
PARP-1	+	-	-	-
Chromatin	-	+	-	+

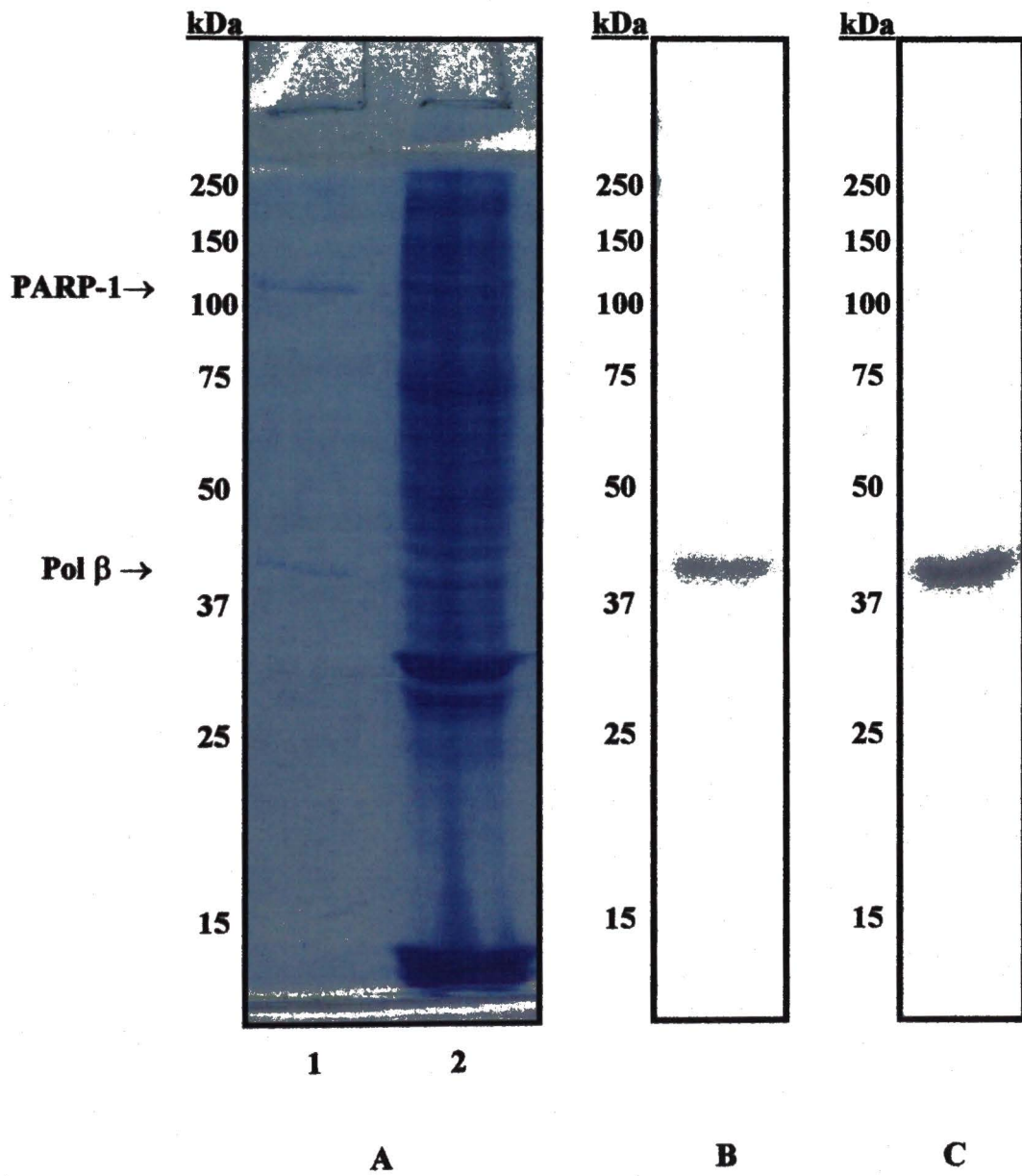


Figure 11. Changes in DNA polymerase β activity as a result of covalent poly(ADP-ribose)ation of PARP-1. Pure pol β protein was subjected to covalent poly(ADP-ribose)ation conditions followed by activity gel assays. Lane 1 displays a single band that indicated the position and enzymatic activity level of control pol β protein. A prior incubation of pol β in buffer containing 100 μM βNAD^+ did not result in a change in DNA polymerase activity (lane 2). The addition of PARP-1 for incubations with either 0.20 μM (lane 3) or 100 μM (lane 4) βNAD^+ are also presented.

Pol β	+	+	+	+
PARP-1	-	-	+	+
[βNAD⁺](μM)	0	100	0.20	100

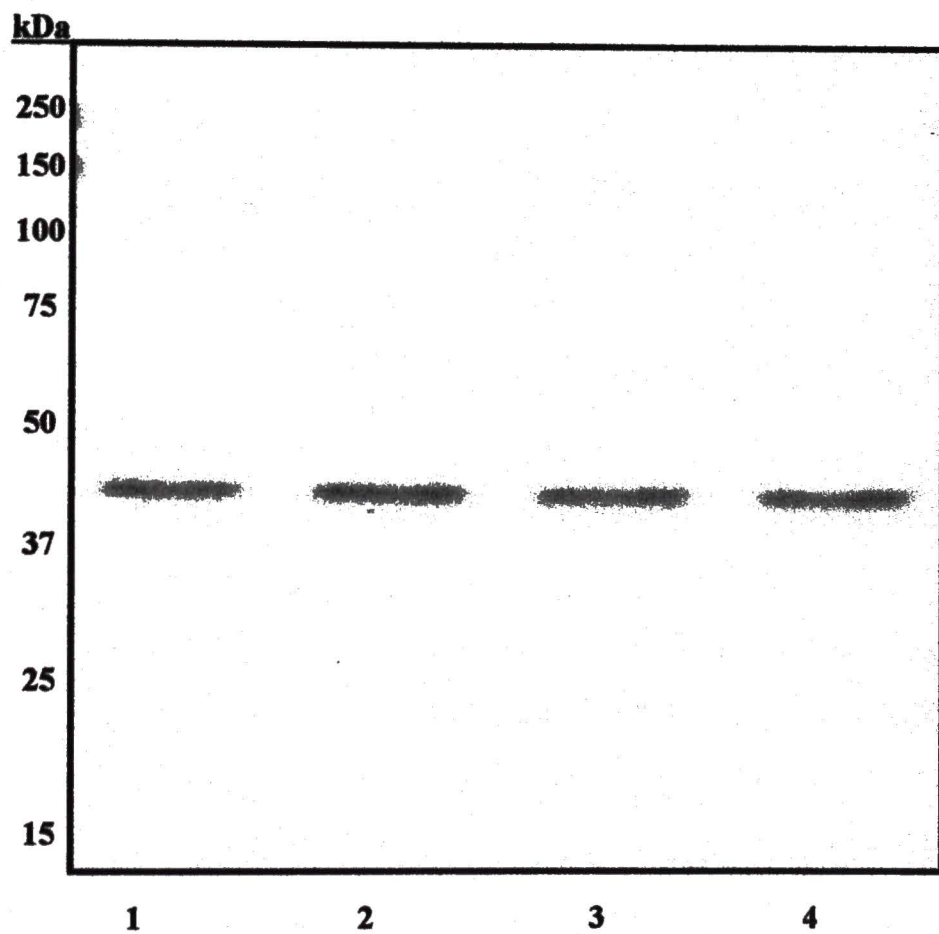


Figure 12. DNA polymerase β activity gels with chromatin extracts following covalent poly(ADP-ribosyl)ation. Chromatin proteins were subjected to DNA polymerase activity gel assays. Rat liver chromatin proteins were resolved by 10% SDS-PAGE and assayed for activity using the activity gel technique (lane 1). Chromatin proteins were also subjected to covalent protein-poly(ADP-ribosyl)ation with 100 μM βNAD^+ prior to assaying for pol β activity (lane 2).

Chromatin	+	+
[βNAD⁺](μM)	-	100

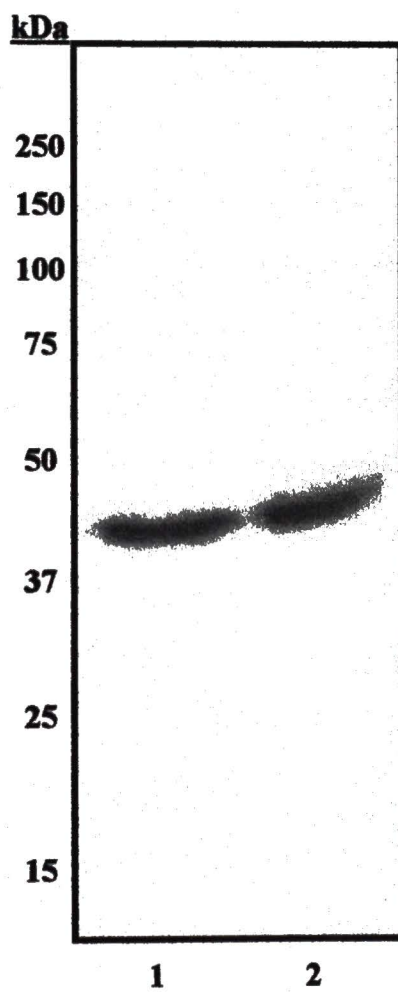
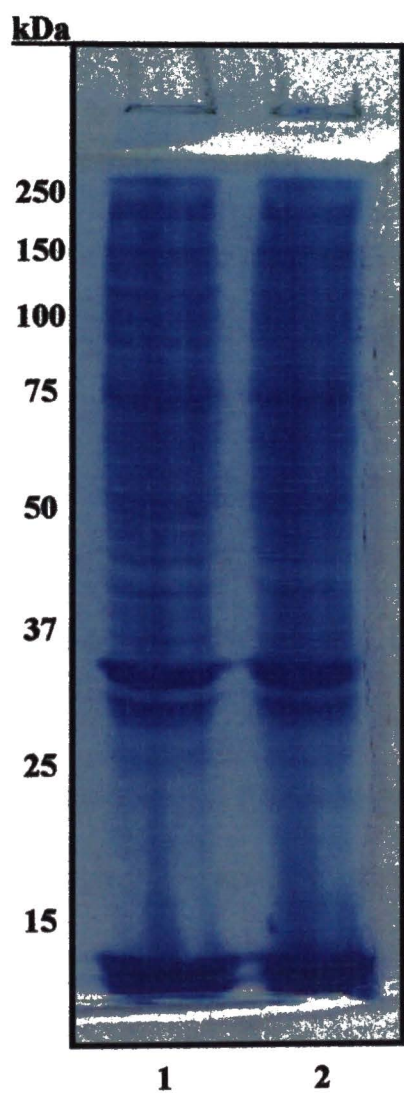


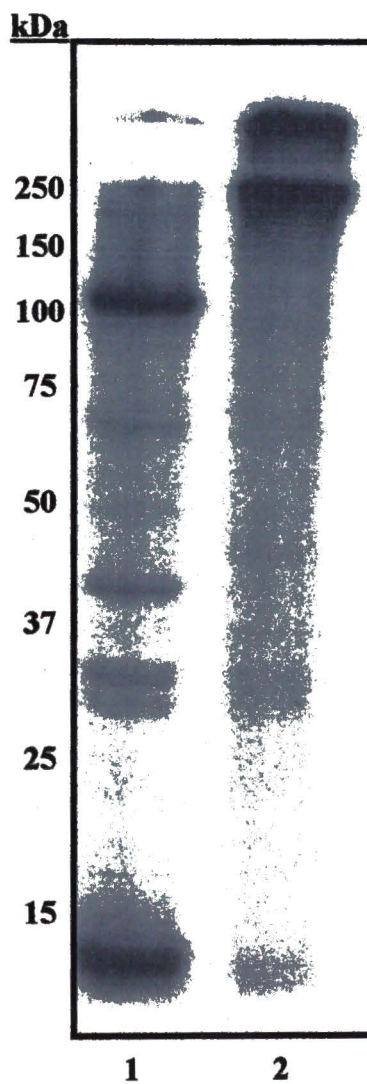
Figure 13. Poly(ADP-ribosyl)ation of chromatin proteins. Chromatin proteins were subjected to poly(ADP-ribosyl)ation conditions at the indicated βNAD^+ concentrations. Samples were electrophoresed by 10% SDS-PAGE, stained with Coomassie blue (13A) and autoradiographed (13B). Incubation with 200nM βNAD^+ resulted in the covalent ADP-riboylation of multiple proteins including the primary acceptor PARP-1 and histones (13B, lane 1). With a 100 μM βNAD^+ concentration, modified proteins were unable to enter the gel as indicated by the presence of a single band at the origin of the gel (lane 2).

Chromatin + +
[β NAD⁺](μ M) 0.20 100

+ +
0.20 100



A



B

Figure 14. PARP-1 activity gels. Pure PARP-1 protein was electrophoresed and assayed by the activity gel technique. Panel 14A, lane 1 is a radioactive band that results from electrophoresis of PARP-1 by 10% SDS-PAGE and *in situ* renaturation. Lane 2 is activity from renatured PARP-1 following electrophoresis of chromatin proteins by identical conditions as for lane 1. Panel 14B is an autoradiogram of chromatin proteins following incubation with radiolabeled βNAD^+ and 10% SDS-PAGE. Panel 14C, lane 1 is chromatin extract that was subjected to protein-poly(ADP-ribosyl)ation conditions in the presence of 0.20 μM radiolabeled βNAD^+ prior to assaying for PARP-1 activity. Lane 2 are results from performing an identical experiment as before yet with 100 μM βNAD^+ .

PARP-1	+	-	-	-	-
Chromatin	-	+	+	+	+
[βNAD⁺](μM)			0.20	0.20	100

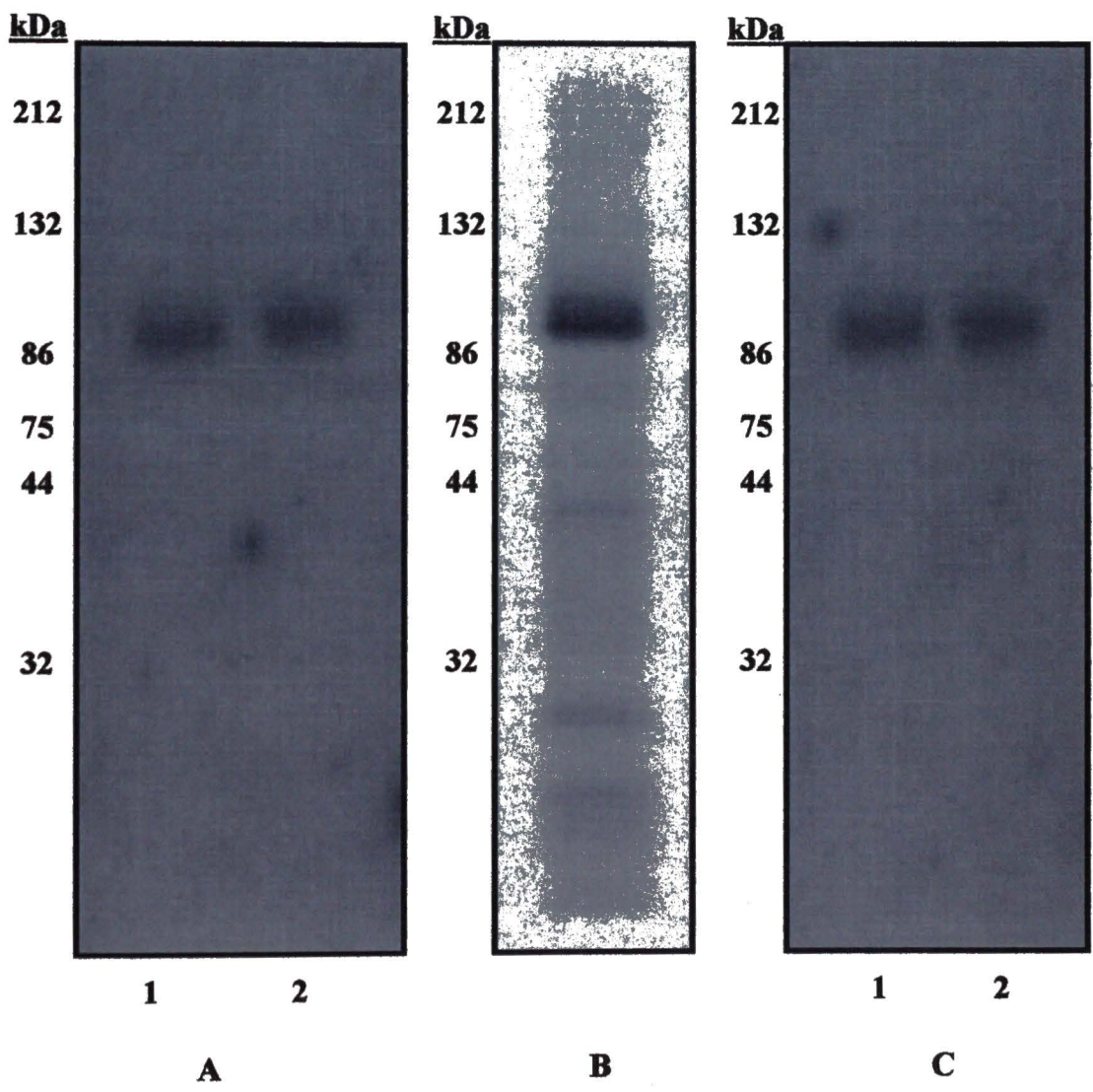
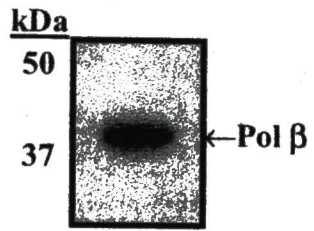


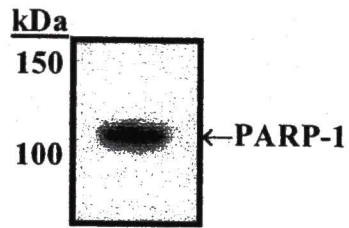
Figure 15. Co-immunoprecipitation of PARP-1 with DNA polymerase β . Pure pol β protein was subjected to immunoprecipitation followed by SDS-PAGE and western blotting using the previously mentioned antibodies (panel 15A). In addition to pol β , PARP-1 was detected in the immunoprecipitated material by western blotting using PARP-1 specific antibodies (panel 15B).

IP: α -Pol β
Western:
 α -Pol β



A

IP: α -Pol β
Western:
 α -PARP-1

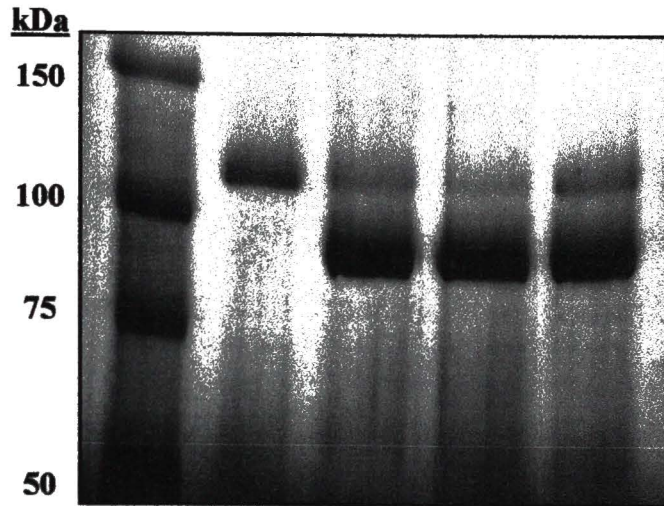


B

Figure 16. Proteolysis of PARP-1 with caspases. Pure caspase-3 and 200 ng of PARP-1 were co-incubated for the indicated times with a molar ratio of 1:10. This incubation was followed by 10% SDS-PAGE and silver staining with results presented in panel 16A. In panel B, identical incubations were performed using caspase-7. In both panels, the first lane is 80 ng of PARP-1 protein not subjected to proteolysis by either caspase and electrophoresed as a control.

A

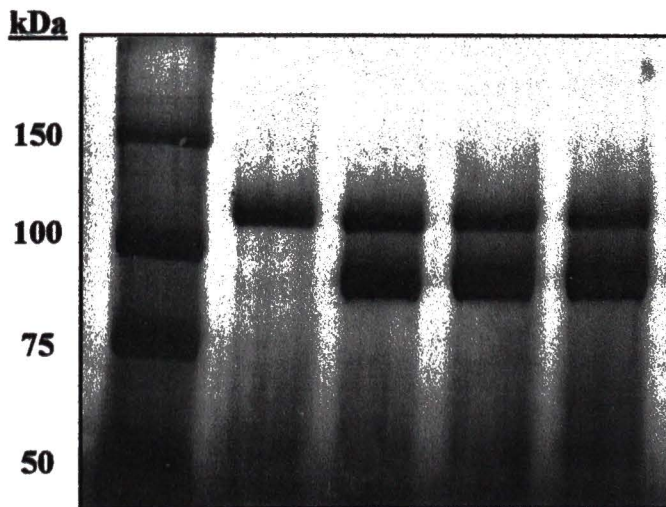
		Con	15	30	240 (min)
Caspase-3	-	-	+	+	+
PARP-1 (ng)	-	80	200	200	200



% Proteolysis		81	87	80
	1	2	3	4

B

		Con	15	30	240 (min)
Caspase-7	-	-	+	+	+
PARP-1 (ng)	-	80	200	200	200



% Proteolysis		53	54	54
	1	2	3	4

Figure 17. Proteolysis of PARP-1 with caspase-3 following poly(ADP-ribosyl)ation. Lane 1 is PARP-1 protein electrophoresed by 10% SDS-PAGE and Coomassie blue stained. PARP-1 protein was incubated with caspase-3 at a molar ratio of 1:10 for 1 hour and electrophoresed and stained as mentioned before. Lanes 3 and 4 are again identical to lane 2 except for the addition of an initial incubation to automodify PARP-1 at the indicated β NAD⁺ concentration prior to caspase-3 proteolysis.

Caspase-3	-	+	+	+
PARP-1	+	+	+	+
βNAD⁺ (μM)	-	-	0.20	100

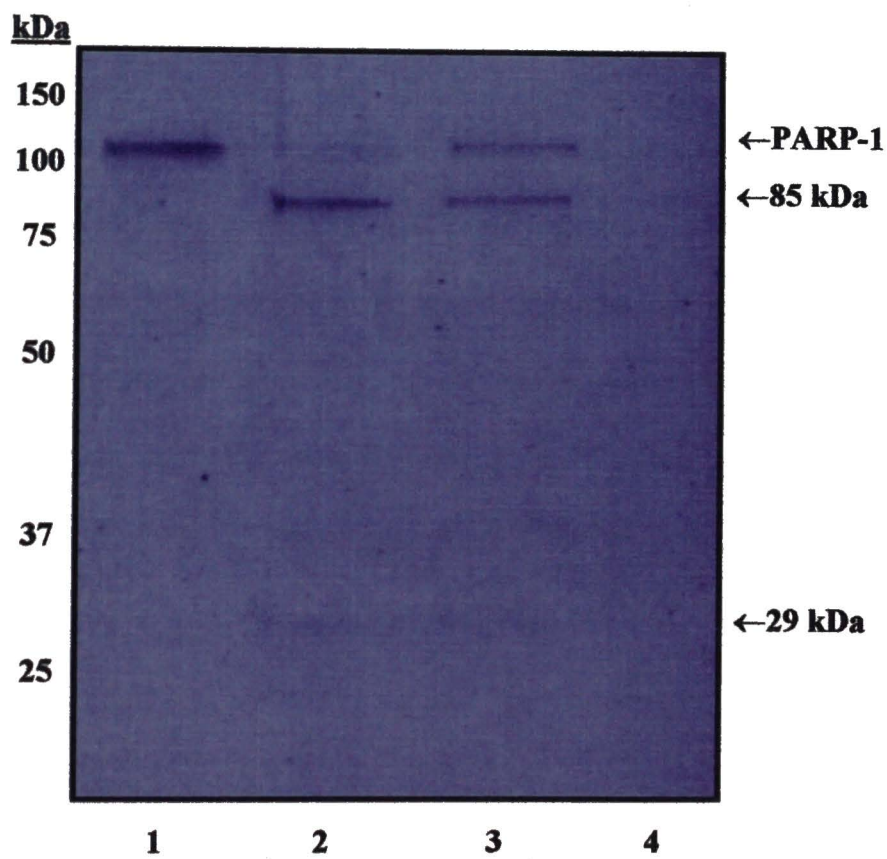
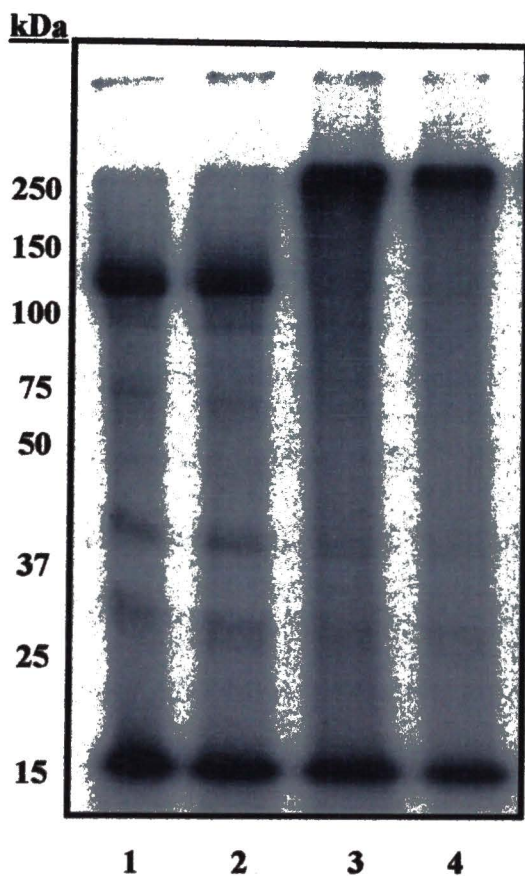


Figure 18. Proteolysis of PARP-1 in chromatin extracts with caspases following protein-poly(ADP-ribosyl)ation. Lane 1 of panel A is provided as a control where chromatin proteins were incubated with 0.20 μM βNAD^+ and then electrophoresed by 10% SDS-PAGE, dried and subjected to autoradiography. Panel A shows caspase-3 incubations with chromatin extracts following poly(ADP-ribosyl)ation at the indicated radiolabeled βNAD^+ concentrations. Panel B are results from identical incubations except with caspase-7. Panels C and D are Coomassie blue stained histone H1 to show equal loading of lanes.

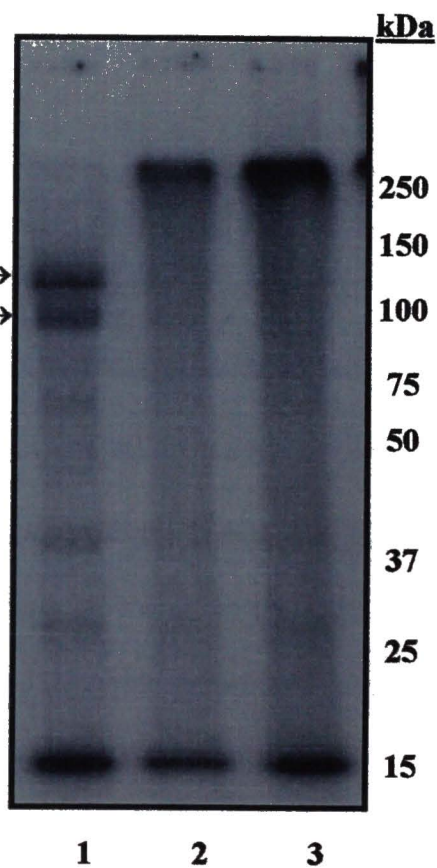
Caspase	-	3	3	3
βNAD⁺ (μM)	0.20	0.20	1.0	100

7	7	7
0.20	1.0	100

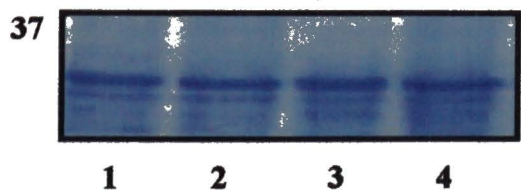


←PARP-1→
← 85 kDa →

A

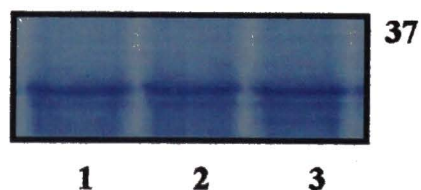


B



←H1→

C



D

Figure 19. Non-specific proteolysis of pol β with trypsin. Lane 1 corresponds to pure native pol β that was electrophoresed by 10% SDS-PAGE and Coomassie blue stained as a negative proteolytic control. Lane 2 is an incubation of trypsin with pol β at a ratio of 1:1000 that did not result in any detectable fragment generation. However, as presented in lane 3, decreasing the enzyme:substrate ratio to 1:10 resulted in tryptic digestion of pol β into two primary fragments of 31 and 8 kDa.

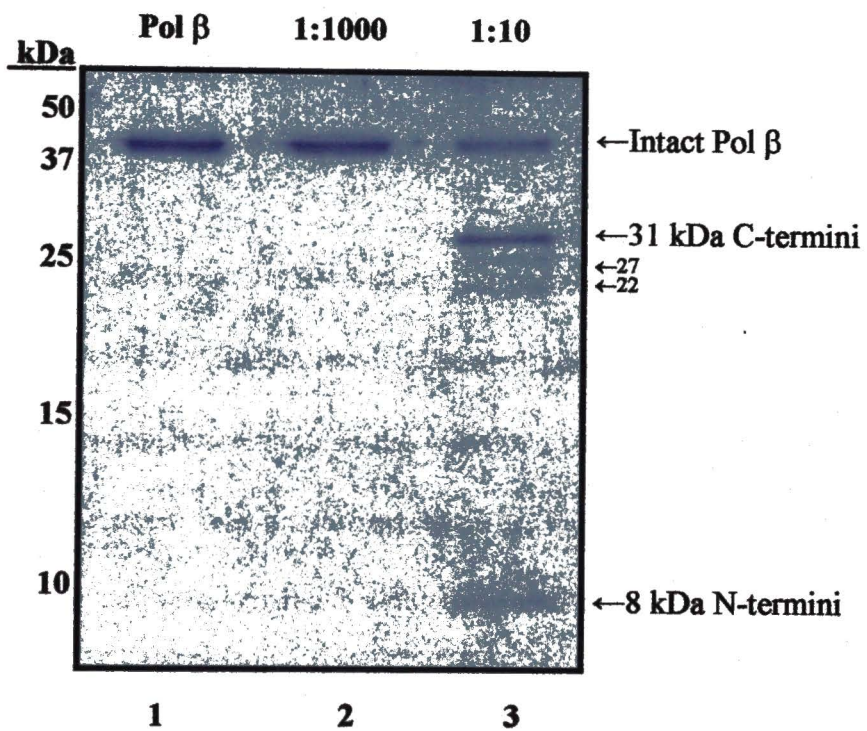


Figure 20. Co-immunoprecipitation of PARP-1 apoptotic peptide fragments with pol β . Pure pol β protein was incubated with caspase-3 generated peptide fragments and then subjected to anti-pol β immunoprecipitation in the absence of antibodies as a negative control (lane 1). This experiment was performed again in the presence of anti-pol β antibodies. The supernatants were collected and are presented as results in lane 2. Immunoprecipitated material were electrophoresed as lane 3. Western blotting for PARP-1 indicated that indeed the 85 and 29 kDA peptides were present in the immunoprecipitated material. (w/o= without antibodies, w/ α =with antibodies)

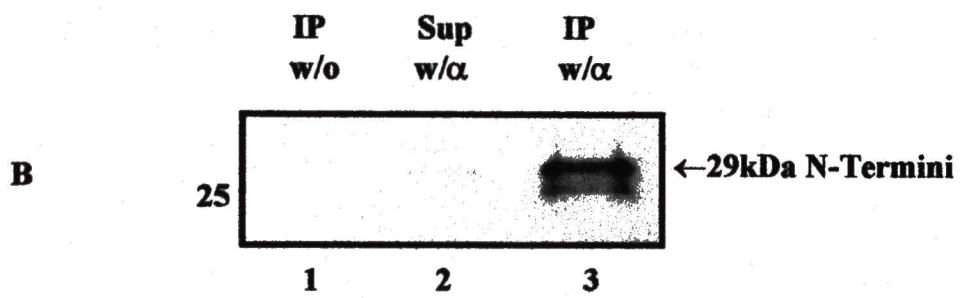
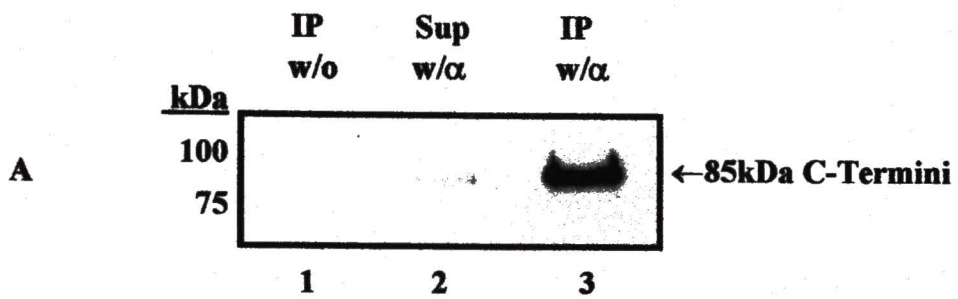
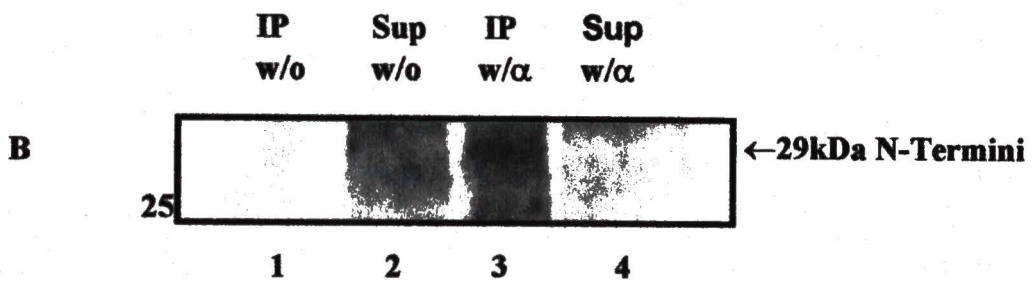
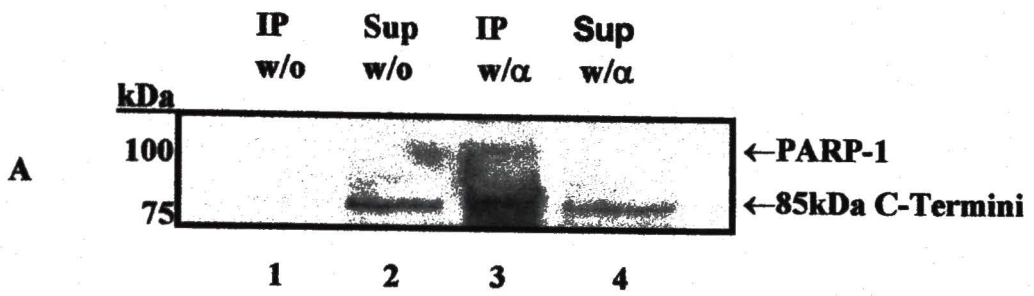


Figure 21. Co-immunoprecipitation of PARP-1 apoptotic peptide fragments with pol β in crude chromatin extracts. Following caspase-7 proteolysis, immunoprecipitation with anti-pol β antibodies was performed followed by 10% SDS-PAGE and western blotting for PARP-1 peptide fragments. Lanes 1 (supernatant) and 2 (precipitate) were performed in the absence of pol β antibodies. This experiment was performed again in the presence of anti-pol β antibodies and resulted in a detectable presence of both PARP-1 apoptotic fragments as well as the intact protein in immunoprecipitated material (lane 3). (w/o=without antibodies, w/ α =with antibodies)



CHAPTER IV

DISCUSSION

In this dissertation results from experiments demonstrate that both caspase-generated peptide fragments of PARP-1 physically interact with pol β . These molecular interactions were significant enough to permit co-immunoprecipitation of both PARP-1 degradation products with pol β when using an *in vitro* system involving purified components (figure 20, lane 3). The ability of pol β to bind each PARP-1 peptide fragment appears to be distinct from results generated with other proteins identified to interact with this DNA polymerase [38]. These results also support the notion that PARP-1 peptide products originating from caspase degradation may physically interact with pol β during the execution phase of apoptosis. Therefore, a mechanism likely exists where inhibition of pol β function(s) results by interaction(s) with the 85 or 29 kDa PARP-1 fragments during apoptotic cell death.

Nonetheless, it must be pointed out that these results generated with co-immunoprecipitation experiments require caution. For example, protocols described above were carried out with non-physiological protein ratios. Co-incubation of these two polymerases was performed with a molecular stoichiometry of 1:1. Under these conditions, PARP-1 co-immunoprecipitation was clearly observed (figure 15B). Surprisingly, the quantity of precipitated PARP-1 protein was sufficient for detection by

western blotting (*vide supra*). Co-immunoprecipitation of pure PARP-1 with pol β was not previously demonstrated by published data, except when using GST-tagged mutant proteins [17]. It cannot be assumed however, that a similar stoichiometry exists between each PARP-1 fragment and pol β following incubations with caspase-3. Since degradation of PARP-1 was calculated to result in nearly 90 percent conversion to product, we also calculated that a 1:1.1 ratio results between pol β and both PARP-1 fragments. Residual caspase substrate (intact PARP-1) was also present at a ratio of 1:10 (enzyme:substrate). Thus, intact PARP-1 may also physically interact with pol β (as shown in figure 15B) yet may remain undetected in precipitated material following incubation with caspase-3 (Figure 20). These findings can be explained in a number of ways. First, the amount of precipitated PARP-1 may be insufficient for detection under the conditions employed here. Alternatively, PARP-1 may compete for pol β binding with either the 85 or 29 kDa fragments. The possibility then exists that competition occurs between intact PARP-1 and the apoptotic peptide. Further, the presence of caspase-3 in solution during immunoprecipitation may provide additional complexities that cannot be explained at this time. For example, it cannot be ruled out that pol β is not a substrate for caspases even though no results are currently available to suggest this. Nonetheless, the lack of intact PARP-1 does not contradict the notion that pol β physically interacts with both apoptotic peptide fragments. Thus observations here provide for interesting speculations that support the previously proposed mechanism where PARP-1 peptide fragments inhibit pol β during the execution phase of apoptosis.

When co-immunoprecipitation experiments were performed with a rat liver chromatin extract, the results again supported the conclusion that physical interactions between pol β and PARP-1 and both apoptotic fragments occurs (figure 21). Though within a chromatin milieu association between these proteins is suggested, as presented in figure 21, other possibilities do exist. Intact PARP-1, both of the fragments and pol β are capable of binding DNA. Therefore, precipitation of pol β could also bring down a chromatin complex and result in detection of PARP-1 related proteins by western blotting. In addition, other proteins are capable of forming physical interactions with both PARP-1 and pol β . This fact may provide a polypeptide scaffold and therefore artifactually induce indirect interactions. An additional complication may also arise when using chromatin extracts since under these conditions the protein ratios were not known prior to experimentation. Nonetheless, prior to proteolytic degradation of PARP-1, a stoichiometry of 1:175 of pol β to PARP-1 was estimated (personal communication with Wilson SH lab, NIEHS, NC). This is a significant difference when compared to incubations performed with purified components. In addition, owing to this estimated physiological ratio, reciprocal co-immunoprecipitations were not performed.

With the proposed model, a situation arises where intact PARP-1 may compete with the 85 or 29 kDa peptides for interactions with pol β . Caspase proteolysis of PARP-1 could then serve as a molecular switch to regulate pol β function(s). In the absence of active caspases, intact PARP-1 would facilitate repair of damaged DNA. However, following proteolysis of PARP-1 by caspases, peptide fragments may inhibit pol β activity and also modulate chromatin fragmentation.

It is also important to mention that when PARP-1 was proteolyzed into peptide fragments by caspase 3 or 7, experiments were run to determine the best conditions for protein digestion. From these results, both proteases were capable of degrading PARP-1 efficiently in an *in vitro* reconstituted system (figure 16, A and B). Although these proteases demonstrated similar kinetics, caspase-3 seems best suited to proteolyze PARP-1 under purified conditions in solution. Therefore, co-immunoprecipitation of pure pol β in the presence of PARP-1 fragments was performed following incubation with caspase-3. In contrast, caspase-7 was determined to be best suited for proteolysis of PARP-1 when using chromatin extracts (figure 18). Experiments involving chromatin extracts and PARP-1 proteolysis were therefore performed following incubations with caspase-7.

Initially, an *in vitro* proteolysis assay for caspase-3 was developed. Using homogeneously pure PARP-1, in the absence of synthesized ADP-ribose polymers, gels were stained with silver (figure 15). This technique provided a high level of sensitivity as required to detect the nanomolar amounts of substrate protein that were used in each reaction. However, when PARP-1 was incubated under automodification conditions prior to caspase proteolysis, silver staining was not used because this procedure results in significant background staining by detection of nucleic acids, including ADP-ribose polymers. Therefore, gels were stained with Coomassie blue as needed to detect protein only (figure 17). When the intent was to address caspase proteolysis of poly(ADP-ribosyl)ated PARP-1, use of radiolabeled β NAD⁺ showed very sensitive detection conditions by autoradiography (figure 18). It should be stated though that when using radiolabeled β NAD⁺, the results generated by autoradiography only indicated the position

of poly(ADP-ribosyl)ated proteins. In other words, a change in the electrophoretic mobility of non-modified proteins was not visible.

Also, this dissertation project initially intended to address the proposed hypothesis from a cellular physiology approach. Therefore, a functional Comet assay was used and cells were treated with an alkylating agent (MNNG) (figure 6). The difference in DNA migration in these experiments was directly related to the increased amount of strand breaks present within the MNNG treated cells. The assay was first presented in 1984 [52] as a procedure to compare the extent of DNA damage in individual cells and was not previously performed in this lab. This method of detecting DNA damage in cells presented a number of shortcomings however. At the time this procedure was performed, measurements were primarily done by hand, thus representing a potential source of error. In addition, a large population of cells must also be sampled. During the course of this study, other DNA polymerases were reported as potential participants in BER [74,23,57]. Alternatively, chemically modified bases may also be repaired, to a lesser extent, by other DNA repair systems (nucleotide excision repair). For these reasons, it was decided that a study addressing PARP-1, pol β and BER required a more direct biochemical approach.

Biochemical assays to detect pol β binding first involved the generation of an EMSA specific for this DNA polymerase. Therefore, a technique was developed to monitor pol β 's ability to bind a specific DNA substrate under carefully controlled experimental conditions. Since this enzyme has been the most studied eukaryotic polymerase in DNA repair, it was feasible to design a specific DNA substrate for pol β . This was accomplished by the synthesis of three independent DNA fragments. First, a

template strand (Tm) consisting of 27 nucleotides was capped on both ends by single guanine residues. Second, primer (P1) and non-primer strands (P2) were also constructed with 11 thymines. In these DNA strands the 5' and 3' ends were capped with cytosine respectively. This capping permitted proper orientation during annealing. The DNA molecule designed also contained a 5-nucleotide single stranded gap between the 3' end of P1 and the 5' end of P2. Further, the 5' end of P2 possessed a phosphate group to facilitate pol β binding to the gapped DNA substrate. To ensure that this residue was retained during radiolabeling, the reaction was carried out with only P1 annealed to Tm. Under these conditions, the DNA substrate was resistant to 5' labeling of Tm by T4 polynucleotide kinase. Obviously, this was facilitated by the kinase requirement for a blunt double stranded DNA end for phosphate residue transfer. Incubation of this DNA probe with pure pol β , followed by electrophoreses under non-denaturing conditions demonstrated the formation of a bimolecular protein-DNA complex (figure 8, lane 2). When this incubation was repeated with chromatin extracts, only two complexes were visible (figure 8, lane 3). Considering the protein composition of these extracts (figure 10A, lane 2), these results were quite surprising. In fact, it was expected that binding of this radiolabeled probe by pol β would not be observable in the presence of chromatin-forming proteins such as histones. The presence of only two bands suggests that indeed pol β interacts with this DNA substrate in a very selective manner. It should be mentioned that the complex formed with chromatin extracts (figure 8, lane 3) was observed at a slightly different electrophoretic position. This variance is likely due to the human recombinant form of pol β expressed and purified from *E. coli* and used in lane 2.

A more likely explanation is the fact that the human gene for pol β encodes a protein with a molecular weight of 41 kDa [1]. This is slightly different when compared to 39 kDa for the rat gene [18].

Although this EMSA technique was not used to address the affects of poly(ADP-ribosyl)ation on pol β binding of the DNA molecule, a number of other issues can be explored. In addition to pol β , the fact that another polypeptide binds this 5-nucleotide gapped probe presents an interesting possibility. When considering that the BER pathway appears to progress as a sequence of chemical reactions, with the DNA lesion handed from one enzyme to the next, the unidentified band may involve another enzyme of this repair system. This would mean that the substrate generated here is not specific for pol β , but selective. Nonetheless, with the combination of DNA molecules that could be engineered, one might contemplate a study to identify proteins complexing with DNA lesions of different chemical structures known to form during the BER pathway. As an example, a mechanism likely exists that selects between single nucleotide and long patch BER. DNA polymerase β is capable of both single nucleotide incorporation and an uncommon DNA polymerization at an abasic site that results in 5' non-template strand displacement [62]. This alternate BER pathway involving incorporation of multiple nucleotides by pol β may be performed by other DNA polymerases though. The reason for a shift to a polymerase other than pol β is unknown. With this technique, two different probes, engineered to possess different DNA chemical structures, could assist in identifying proteins that bind these nucleic acids from a chromatin milieu. Further, this

technique would be reasonable for application with mutated pol β proteins to determine changes in affinity for a DNA substrate.

Also in this dissertation project, similar activity gels were performed with specificity for either pol β or PARP-1. Though this technique requires the denaturation of polypeptides prior to electrophoresis, sufficient protein was chemically renatured *in situ* to form conformationally active enzymes capable of polymerizing nucleic acids. This characteristic provided a technique to select for either enzyme from a myriad of chromatin proteins. In addition, the absence of a visible change in activity levels for pol β following poly(ADP-ribosyl)ation of chromatin proteins suggested that only a small percentage of this polymerase was covalently modified by the polymer. Another possibility is that within a chromatin environment, pol β is not a substrate. Either situation provides for interesting questions to be addressed. To illustrate, if pol β is not an acceptor for poly(ADP-ribose) in this chromatin environment, under what conditions is it, or is the *in vitro* results previously generated within this lab artifactual? This latter statement is however unlikely for a number of reasons and refutable by results presented in figure 13B, lane 1 where the radioactive band at 40 kDa is likely to be pol β .

In summary, this dissertation project examined the effects of poly(ADP-ribosyl)ation on pol β activity. These results were not in disagreement with previous work performed by other labs [51,17]. However, the number of pol β proteins covalently modified by PARP-1 is believed to be only a small fraction of the total when poly(ADP-ribosyl)ated under the conditions used here. This is in agreement with results generated when assaying for PARP-1 activity by the same technique. However, further

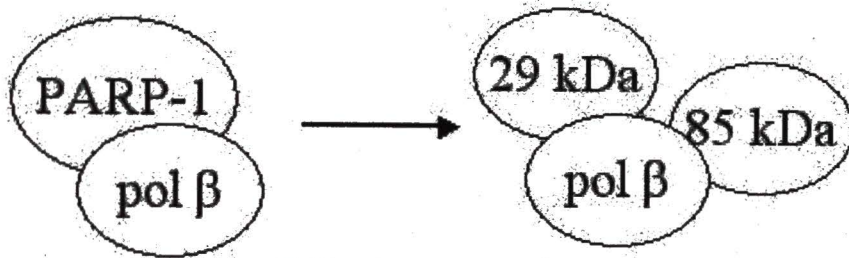
experimentation is required to determine the role of PARP-1 in regulating the function(s) of pol β at the biochemical level. PARP-1 was also demonstrated to co-immunoprecipitate with pol β . Interactions between pol β and the caspase generated PARP-1 peptide fragments were also shown. These results provide for the proposal of a mechanism that might facilitate apoptosis. Upon activation of caspases 3 and 7, PARP-1 is proteolyzed. This proteolysis occurs primarily by caspase-3 degrading non-(ADP-ribosyl)ated PARP-1. In addition, caspase-7 proteolyzes those PARP-1 molecules present in a modified form. The resulting PARP-1 peptide fragments interact with pol β and inhibit DNA repair that would stand in opposition to apoptosis related chromatin degradation. PARP-1 is then part of a cellular switch facilitating DNA repair yet serving to irreversibly favor apoptosis (figure 22). This control by PARP-1 of cell death may reside in protein-protein interactions with key DNA repair proteins such as pol β [7].

Figure 22. Proposed model for PARP-1 as a switch between DNA repair and cell death.

DNA Repair

Apoptosis

Caspase
Activation



Biochemical
Switch

Competent BER

Pro-Cell Death

CHAPTER V

CONCLUSIONS

PARP-1 modulates BER and appears to also alter the progression of apoptosis toward an irreversible state. This regulatory role for PARP-1 in DNA damage repair, and possibly apoptosis, is likely to reside in the regulation of pol β . To test this hypothesis, experiments were performed to address the effects of PARP-1 mediated protein poly(ADP-ribosylation) on the pol β DNA synthesis activity. The results of this investigation support the following conclusions:

1. Though pol β is a substrate for PARP-1, this ADP-ribose polymerase is the primary acceptor for covalent addition of poly(ADP-ribose). This finding suggests that automodification of PARP-1, as opposed to heteromodification of pol β , are the primary chemical reactions catalyzed by PARP-1 to modulate BER activity. These findings are important because DNA polymerase β is responsible for the rate limiting enzymatic reaction in BER with associated regulatory mechanisms possibly providing a target to effect changes in repair proficiency. Additional studies are required to address the role of poly(ADP-ribose) in BER.

2. PARP-1 is a substrate for both apoptotic caspases-3 and 7. This conclusion requires further explanation though. Upon catalytic activation in the presence of DNA strand breaks PARP-1 molecules also serve as covalent acceptors for poly(ADP-ribose). This chemical modification results in a heterogeneous population of PARP-1. The results of this investigation indicate that caspase-3 and caspase-7 serve in a similar fashion to proteolyze PARP-1 molecules that, respectively, may be free of ADP-ribose polymer or covalently modified. This finding is important because a fraction of PARP-1 molecules are believed to possess poly(ADP-ribose) at any given time. Accordingly, PARP-1 cleavage requires either a single protease capable of recognizing multiple substrates or multiple proteases, the later being the case. Taken further, this overlap in caspase function clearly supports the cellular importance of the proteolytic degradation of PARP-1 during the execution phase of apoptosis and necessitates a more intensive biochemical investigation of these apoptotic caspases with PARP-1 substrate molecules.

3. The caspase-generated peptide fragments of PARP-1 independently retain the ability to physically associate with pol β . PARP-1 proteolysis is a hallmark event signaling cellular entry into the irreversible and final stage of apoptosis. Both peptide fragments of PARP-1 are known to retain domain-specific functions associated with the intact enzyme. These interactions are then relevant to understanding how a cell transforms from supporting genome integrity toward promoting chromatin degradation, and may reside in activity retained within the PARP-1 peptide fragments. In regard to this investigation, this is exemplified by changes in physical association with pol β . Further research is then

required to determine if other mechanisms exist that facilitate an irreversible cellular switch to apoptosis.

The results presented here support a proposed mechanism that may serve to mediate this irreversible switch of a cell from repair directed, to an apoptotic state. Following excessive DNA damage PARP-1 promotes DNA repair by automodification. Should apoptotic pathways predominate and caspase proteolysis ensue, PARP-1 degradation occurs, and as a result, synthesis of ADP-ribose polymer would be attenuated. By physical association of the resulting peptide fragments of PARP-1 with pol β , the cell is shifted from pro-survival, with DNA repair, to pro-death, with chromatin fragmentation. This switch results from changes in protein-protein interactions for PARP-1 with pol β . Thus, the results of this investigation implicate PARP-1 key mediator in effecting a cellular switch toward an irreversible apoptotic state.

REFERENCES

1. Abbotts, J., D. N. SenGupta, et al. (1988). "Expression of human DNA polymerase beta in *Escherichia coli* and characterization of the recombinant enzyme." *Biochemistry* 27(3): 901-9.
2. Alvarez-Gonzalez, R. (1994). "DeoxyNAD and deoxyADP-ribosylation of proteins." *Mol Cell Biochem* 138(1-2): 213-9.
3. Alvarez-Gonzalez, R., H. Spring, et al. (1999). "Selective loss of poly(ADP-ribose) and the 85-kDa fragment of poly(ADP-ribose) polymerase in nucleoli during alkylation-induced apoptosis of HeLa cells." *J Biol Chem* 274(45): 32122-6.
4. Bennett, R. A., D. M. Wilson, 3rd, et al. (1997). "Interaction of human apurinic endonuclease and DNA polymerase beta in the base excision repair pathway." *Proc Natl Acad Sci U S A* 94(14): 7166-9.
5. Beard, W. A., S. H. Wilson. (2000). "Structural design of a eukaryotic DNA polymerase: DNA polymerase beta." *Mutat Res* (3-4): 231-44.

6. Beneke, S., R. Alvarez-Gonzalez, A. Burkle. (2000). "Comparative characterization of poly(ADP-ribose) polymerase-1 from two mammalian species with different life span." *Exp Gerontol* 35(8): 989-1002.
7. Bernstein, C., H. Bernstein, et al. (2002). "DNA repair/pro-apoptotic dual-role proteins in five major DNA repair pathways: fail-safe protection against carcinogenesis." *Mutat Res* 511(2): 145-78.
8. Bork, P., K. Hofmann, et al. (1997). "A superfamily of conserved domains in DNA damage-responsive cell cycle checkpoint proteins." *Faseb J* 11(1): 68-76.
9. Brightwell, M. and S. Shall (1971). "Poly(adenosine diphosphate ribose) polymerase in *Physarum polycephalum* nuclei." *Biochem J* 125(3): 67P.
10. Burkle, A. (2001). "Poly(ADP-ribosyl)ation, a DNA damage-driven protein modification and regulator of genomic instability." *Cancer Lett* 163(1): 1-5.
11. Casas-Finet, J. R., A. Kumar, et al. (1992). "Mammalian DNA polymerase beta: characterization of a 16-kDa transdomain fragment containing the nucleic acid-binding activities of the native enzyme." *Biochemistry* 31(42): 10272-80.

12. Chambon, P., J. D. Weill, et al. (1963). "Nicotinamide mononucleotide activation of new DNA-dependent polyadenylic acid synthesizing nuclear enzyme." *Biochem Biophys Res Commun* 11: 39-43.
13. Chang, W. J. and R. Alvarez-Gonzalez (2001). "The sequence-specific DNA binding of NF-kappa B is reversibly regulated by the automodification reaction of poly (ADP-ribose) polymerase 1." *J Biol Chem* 276(50): 47664-70.
14. Chen, L., K. Trujillo, et al. (2000). "Interactions of the DNA ligase IV-XRCC4 complex with DNA ends and the DNA-dependent protein kinase." *J Biol Chem* 275(34): 26196-205.
15. D'Amours, D., M. Germain, et al. (1998). "Proteolysis of poly(ADP-ribose) polymerase by caspase 3: kinetics of cleavage of mono(ADP-ribosyl)ated and DNA-bound substrates." *Radiat Res* 150(1): 3-10.
16. D'Amours, D., F. R. Sallmann, et al. (2001). "Gain-of-function of poly(ADP-ribose) polymerase-1 upon cleavage by apoptotic proteases: implications for apoptosis." *J Cell Sci* 114(Pt 20): 3771-8.

17. Dantzer, F., G. de La Rubia, et al. (2000). "Base excision repair is impaired in mammalian cells lacking Poly(ADP-ribose) polymerase-1." *Biochemistry* 39(25): 7559-69.
18. Date, T., M. Yamaguchi, et al. (1988). "Expression of active rat DNA polymerase beta in *Escherichia coli*." *Biochemistry* 27(8): 2983-90.
19. Donepudi, M. and M. G. Grutter (2002). "Structure and zymogen activation of caspases." *Biophys Chem* 101-102: 145-53.
20. Fernandes-Alnemri, T., G. Litwack, et al. (1994). "CPP32, a novel human apoptotic protein with homology to *Caenorhabditis elegans* cell death protein Ced-3 and mammalian interleukin-1 beta-converting enzyme." *J Biol Chem* 269(49): 30761-4.
21. Fernandes-Alnemri, T., A. Takahashi, et al. (1995). "Mch3, a novel human apoptotic cysteine protease highly related to CPP32." *Cancer Res* 55(24): 6045-52.
22. Fortini, P., E. Parlanti, et al. (1999). "The type of DNA glycosylase determines the base excision repair pathway in mammalian cells." *J Biol Chem* 274(21): 15230-6.

23. Fortini, P., B. Pascucci, et al. (1998). "Different DNA polymerases are involved in the short- and long-patch base excision repair in mammalian cells." *Biochemistry* 37(11): 3575-80.
24. Friedberg, E. C., G. C. Walker, et al. (1997). "DNA repair and mutagenesis." ASM Press.
25. Gary, R., K. Kim, et al. (1999). "Proliferating cell nuclear antigen facilitates excision in long-patch base excision repair." *J Biol Chem* 274(7): 4354-63.
26. Germain, M., E. B. Affar, et al. (1999). "Cleavage of automodified poly(ADP-ribose) polymerase during apoptosis. Evidence for involvement of caspase-7." *J Biol Chem* 274(40): 28379-84.
27. Ikejima, M., S. Noguchi, et al. (1990). "The zinc fingers of human poly(ADP-ribose) polymerase are differentially required for the recognition of DNA breaks and nicks and the consequent enzyme activation. Other structures recognize intact DNA." *J Biol Chem* 265(35): 21907-13.
28. Jakoby, W. B., I. H. Pastan. (1979). "Cell culture." Academic Press.

29. Janicke, R. U., P. Ng, et al. (1998). "Caspase-3 is required for alpha-fodrin cleavage but dispensable for cleavage of other death substrates in apoptosis." *J Biol Chem* 273(25): 15540-5.
30. Jezewska, M. J., R. Galletto, et al. (2003). "Rat polymerase beta gapped DNA interactions: antagonistic effects of the 5' terminal PO₄ - group and magnesium on the enzyme binding to the gapped DNAs with different ssDNA gaps." *Cell Biochem Biophys* 38(2): 125-60.
31. Jezewska, M. J., S. Rajendran, et al. (2001). "Interactions of the 8-kDa domain of rat DNA polymerase beta with DNA." *Biochemistry* 40(11): 3295-307.
32. Juan, T. S., I. K. McNiece, et al. (1997). "Identification and mapping of Casp7, a cysteine protease resembling CPP32 beta, interleukin-1 beta converting enzyme, and CED-3." *Genomics* 40(1): 86-93.
33. Kameshita, I., Z. Matsuda, et al. (1984). "Poly (ADP-Ribose) synthetase. Separation and identification of three proteolytic fragments as the substrate-binding domain, the DNA-binding domain, and the automodification domain." *J Biol Chem* 259(8): 4770-6.

34. Kubota, Y., R. A. Nash, et al. (1996). "Reconstitution of DNA base excision-repair with purified human proteins: interaction between DNA polymerase beta and the XRCC1 protein." *Embo J* 15(23): 6662-70.
35. Kuida, K., T. S. Zheng, et al. (1996). "Decreased apoptosis in the brain and premature lethality in CPP32-deficient mice." *Nature* 384(6607): 368-72.
36. Kumar, A., J. Abbotts, et al. (1990). "Identification and properties of the catalytic domain of mammalian DNA polymerase beta." *Biochemistry* 29(31): 7156-9.
37. Kumar, A., S. G. Widen, et al. (1990). "Studies of the domain structure of mammalian DNA polymerase beta. Identification of a discrete template binding domain." *J Biol Chem* 265(4): 2124-31.
38. Kumari, S. R., H. Mendoza-Alvarez, et al. (1998). "Functional interactions of p53 with poly(ADP-ribose) polymerase (PARP) during apoptosis following DNA damage: covalent poly(ADP-ribosyl)ation of p53 by exogenous PARP and noncovalent binding of p53 to the M(r) 85,000 proteolytic fragment." *Cancer Res* 58(22): 5075-8.

39. Le Page, F., V. Schreiber, et al. (2003). "Poly(ADP-ribose) polymerase-1 (PARP-1) is required in murine cell lines for base excision repair of oxidative DNA damage in the absence of DNA polymerase beta." *J Biol Chem* 278(20): 18471-7.
40. Lindahl, T. (1993). "Instability and decay of the primary structure of DNA." *Nature* 362(6422): 709-15.
41. Mahajan, P. B. and Z. Zuo (1998). "Purification and cDNA cloning of maize Poly(ADP)-ribose polymerase." *Plant Physiol* 118(3): 895-905.
42. Matsumoto, Y. and K. Kim (1995). "Excision of deoxyribose phosphate residues by DNA polymerase beta during DNA repair." *Science* 269(5224): 699-702.
43. Mazen, A., J. Menissier-de Murcia, et al. (1989). "Poly(ADP-ribose)polymerase: a novel finger protein." *Nucleic Acids Res* 17(12): 4689-98.
44. Mendoza-Alvarez, H. and R. Alvarez-Gonzalez (1993). "Poly(ADP-ribose) polymerase is a catalytic dimer and the automodification reaction is intermolecular." *J Biol Chem* 268(30): 22575-80.

45. Mendoza-Alvarez, H. and R. Alvarez-Gonzalez (1999). "Biochemical characterization of mono(ADP-ribosyl)ated poly(ADP-ribose) polymerase." *Biochemistry* 38(13): 3948-53.
46. Menegazzi, M., G. Grassi-Zucconi, et al. (1991). "Differential expression of poly(ADP-ribose) polymerase and DNA polymerase beta in rat tissues." *Exp Cell Res* 197(1): 66-74.
47. Mol, C. D., T. Izumi, et al. (2000). "DNA-bound structures and mutants reveal abasic DNA binding by APE1 and DNA repair coordination [corrected]." *Nature* 403(6768): 451-6.
48. de Murcia G., S. Shall. (2000) "Poly(ADP-ribosyl)ation reactions: from DNA damage and stress signaling to cell death." Oxford University Press.
49. Nash, R. A., K. W. Caldecott, et al. (1997). "XRCC1 protein interacts with one of two distinct forms of DNA ligase III." *Biochemistry* 36(17): 5207-11.
50. Nicholson, D. W., A. Ali, et al. (1995). "Identification and inhibition of the ICE/CED-3 protease necessary for mammalian apoptosis." *Nature* 376(6535): 37-43.

51. Ohashi, Y., A. Itaya, et al. (1986). "Poly(ADP-ribosyl)ation of DNA polymerase beta in vitro." *Biochem Biophys Res Commun* 140(2): 666-73.
52. Ostling, O. and K. J. Johanson (1984). "Microelectrophoretic study of radiation-induced DNA damages in individual mammalian cells." *Biochem Biophys Res Commun* 123(1): 291-8.
53. Pascucci, B., M. Stucki, et al. (1999). "Long patch base excision repair with purified human proteins. DNA ligase I as patch size mediator for DNA polymerases delta and epsilon." *J Biol Chem* 274(47): 33696-702.
54. Pelletier, H. and M. R. Sawaya (1996). "Characterization of the metal ion binding helix-hairpin-helix motifs in human DNA polymerase beta by X-ray structural analysis." *Biochemistry* 35(39): 12778-87.
55. Pelletier, H., M. R. Sawaya, et al. (1994). "Structures of ternary complexes of rat DNA polymerase beta, a DNA template-primer, and ddCTP." *Science* 264(5167): 1891-903.
56. Pelletier, H., M. R. Sawaya, et al. (1996). "Crystal structures of human DNA polymerase beta complexed with DNA: implications for catalytic mechanism, processivity, and fidelity." *Biochemistry* 35(39): 12742-61.

57. Podlutzky, A. J., Dianova, II, et al. (2001). "Human DNA polymerase beta initiates DNA synthesis during long-patch repair of reduced AP sites in DNA." *Embo J* 20(6): 1477-82.
58. Podlutzky, A. J., Dianova, II, et al. (2001). "DNA synthesis and dRPase activities of polymerase beta are both essential for single-nucleotide patch base excision repair in mammalian cell extracts." *Biochemistry* 40(3): 809-13.
59. Prasad, R., W. A. Beard, et al. (1998). "Functional analysis of the amino-terminal 8-kDa domain of DNA polymerase beta as revealed by site-directed mutagenesis. DNA binding and 5'-deoxyribose phosphate lyase activities." *J Biol Chem* 273(18): 11121-6.
60. Prasad, R., W. A. Beard, et al. (1998). "Human DNA polymerase beta deoxyribose phosphate lyase. Substrate specificity and catalytic mechanism." *J Biol Chem* 273(24): 15263-70.
61. Prasad, R., G. L. Dianov, et al. (2000). "FEN1 stimulation of DNA polymerase beta mediates an excision step in mammalian long patch base excision repair." *J Biol Chem* 275(6): 4460-6.

62. Prasad, R., O. I. Lavrik, et al. (2001). "DNA polymerase beta -mediated long patch base excision repair. Poly(ADP-ribose)polymerase-1 stimulates strand displacement DNA synthesis." *J Biol Chem* 276(35): 32411-4.
63. Prasad, R., R. K. Singhal, et al. (1996). "Specific interaction of DNA polymerase beta and DNA ligase I in a multiprotein base excision repair complex from bovine testis." *J Biol Chem* 271(27): 16000-7.
64. Rotonda, J., D. W. Nicholson, et al. (1996). "The three-dimensional structure of apopain/CPP32, a key mediator of apoptosis." *Nat Struct Biol* 3(7): 619-25.
65. Sawaya, M. R., R. Prasad, et al. (1997). "Crystal structures of human DNA polymerase beta complexed with gapped and nicked DNA: evidence for an induced fit mechanism." *Biochemistry* 36(37): 11205-15.
66. Simonin, F., L. Hofferer, et al. (1993). "The carboxyl-terminal domain of human poly(ADP-ribose) polymerase. Overproduction in *Escherichia coli*, large scale purification, and characterization." *J Biol Chem* 268(18): 13454-61.
67. Singhal, R. K. and S. H. Wilson (1993). "Short gap-filling synthesis by DNA polymerase beta is processive." *J Biol Chem* 268(21): 15906-11.

68. Slee, E. A., C. Adrain, et al. (2001). "Executioner caspase-3, -6, and -7 perform distinct, non-redundant roles during the demolition phase of apoptosis." *J Biol Chem* 276(10): 7320-6.
69. Slee, E. A., M. T. Harte, et al. (1999). "Ordering the cytochrome c-initiated caspase cascade: hierarchical activation of caspases-2, -3, -6, -7, -8, and -10 in a caspase-9-dependent manner." *J Cell Biol* 144(2): 281-92.
70. Smulson, M. E., D. Pang, et al. (1998). "Irreversible binding of poly(ADP)ribose polymerase cleavage product to DNA ends revealed by atomic force microscopy: possible role in apoptosis." *Cancer Res* 58(16): 3495-8.
71. Soldani, C. and A. I. Scovassi (2002). "Poly(ADP-ribose) polymerase-1 cleavage during apoptosis: an update." *Apoptosis* 7(4): 321-8.
72. Srivastava, D. K., B. J. Berg, et al. (1998). "Mammalian abasic site base excision repair: Identification of the reaction sequence and rate-determining steps." *J Biol Chem* 273(33): 21203-9.
73. Stennicke, H. R. and G. S. Salvesen (1997). "Biochemical characteristics of caspases-3, -6, -7, and -8." *J Biol Chem* 272(41): 25719-23.

74. Stucki, M., B. Pascucci, et al. (1998). "Mammalian base excision repair by DNA polymerases delta and epsilon." *Oncogene* 17(7): 835-43.
75. Talanian, R. V., C. Quinlan, et al. (1997). "Substrate specificities of caspase family proteases." *J Biol Chem* 272(15): 9677-82.
76. Tice, R. R., E. Agurell, et al. (2000). "Single cell gel/comet assay: guidelines for in vitro and in vivo genetic toxicology testing." *Environ Mol Mutagen* 35(3): 206-21.
77. Tomkinson, A. E., L. Chen, et al. (2001). "Completion of base excision repair by mammalian DNA ligases." *Prog Nucleic Acid Res Mol Biol* 68: 151-64.
78. Uchida, K., T. Morita, et al. (1987). "Nucleotide sequence of a full-length cDNA for human fibroblast poly(ADP-ribose) polymerase." *Biochem Biophys Res Commun* 148(2): 617-22.
79. Vispe, S., T. M. Yung, et al. (2000). "A cellular defense pathway regulating transcription through poly(ADP-ribosyl)ation in response to DNA damage." *Proc Natl Acad Sci U S A* 97(18): 9886-91.
80. Wilson, S. H. and T. A. Kunkel (2000). "Passing the baton in base excision repair." *Nat Struct Biol* 7(3): 176-8.

HECKMAN
BINDERY, INC.
Bound-to-Pleas®
NOV 04
N. MANCHESTER, INDIANA 46962

